

# NAVAL POSTGRADUATE SCHOOL

## Monterey, California



### THESIS

**PSPICE SIMULATION OF TOTAL DOSE  
EFFECTS ON COMPOSITE AND SINGLE  
OPERATIONAL AMPLIFIERS**

by

Rebecca Lynne Baczuk

September, 1994

Thesis Advisor:

Sherif Michael

Approved for public release; distribution is unlimited.

19960202 018

DTIC QUALITY INSPECTED 1

<b>REPORT DOCUMENTATION PAGE</b>			Form Approved OMB No. 0704	
Public reporting burden for this collection of information is estimated to average 1 hour per response, including the time for reviewing instruction, searching existing data sources, gathering and maintaining the data needed, and completing and reviewing the collection of information. Send comments regarding this burden estimate or any other aspect of this collection of information, including suggestions for reducing this burden, to Washington headquarters Services, Directorate for Information Operations and Reports, 1215 Jefferson Davis Highway, Suite 1204, Arlington, VA 22202-4302, and to the Office of Management and Budget, Paperwork Reduction Project (0704-0188) Washington DC 20503.				
1. AGENCY USE ONLY (Leave blank)		2. REPORT DATE September 1994		3. REPORT TYPE AND DATES COVERED Master's Thesis
4. TITLE AND SUBTITLE: PSPICE SIMULATION OF TOTAL DOSE EFFECTS ON COMPOSITE AND SINGLE OPERATIONAL AMPLIFIERS (U)			5. FUNDING NUMBERS	
6. AUTHOR(S) Baczuk, Rebecca Lynne				
7. PERFORMING ORGANIZATION NAME(S) AND ADDRESS(ES) Naval Postgraduate School Monterey CA 93943-5000			8. PERFORMING ORGANIZATION REPORT NUMBER	
9. SPONSORING/MONITORING AGENCY NAME(S) AND ADDRESS(ES)			10. SPONSORING/MONITORING AGENCY REPORT NUMBER	
11. SUPPLEMENTARY NOTES The views expressed in this thesis are those of the author and do not reflect the official policy or position of the Department of Defense or the U.S. Government.				
12a. DISTRIBUTION/AVAILABILITY STATEMENT Approved for public release; distribution unlimited			12b. DISTRIBUTION CODE A	
13. ABSTRACT (maximum 200 words) In this research, continuing evidence that composite operational amplifiers perform better than single amplifiers in both gain bandwidth product and slewrate is presented through an approach of using computer simulation to predict ionizing radiation degradation. This technique examines the use of varying transistor parameters within PSPICE modeled composite and single operational amplifier circuits in order to simulate ionizing radiation. A comparison of the results of this simulation with those of previous research, in which composite and single operational amplifiers were irradiated with a LINAC, verifies that this simulation technique provides a reasonable prediction of a response to ionizing radiation for circuits comprised of radiation hardened components. And, in the process of validating this technique, these simulation results verify that composite operational amplifiers offer an improved bandwidth and a faster slewrate compared to single operational amplifiers.				
14. SUBJECT TERMS Ionizing Radiation, Operational Amplifiers, PSPICE			15. NUMBER OF PAGES 87	
			16. PRICE CODE	
17. SECURITY CLASSIFICATION OF REPORT  Unclassified	18. SECURITY CLASSIFICATION OF THIS PAGE  Unclassified	19. SECURITY CLASSIFICATION OF ABSTRACT  Unclassified	20. LIMITATION OF ABSTRACT UL	

NSN 7540-01-280-5500

Standard Form 298 (Rev. 2-89)  
Prescribed by ANSI Std. Z39-18

Approved for public release; distribution is unlimited.

PSPICE Simulation of Total Dose Effects  
on Composite and Single Operational Amplifiers

by

Rebecca L. Baczuk  
Lieutenant, United States Navy  
B.S., United States Naval Academy, 1986

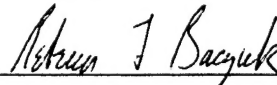
Submitted in partial fulfillment  
of the requirements for the degree of

MASTER OF SCIENCE IN ELECTRICAL ENGINEERING

from the

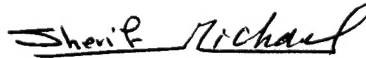
NAVAL POSTGRADUATE SCHOOL  
September 1994

Author:

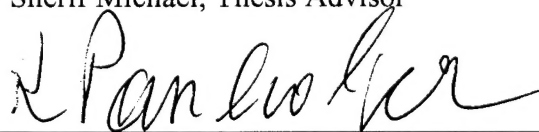


Rebecca L. Baczuk

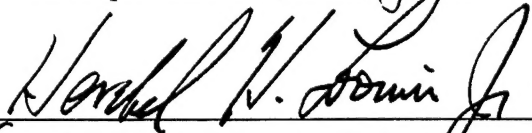
Approved by:



Sherif Michael, Thesis Advisor



Rudolph Panholzer, Second Reader



for Michael A. Morgan, Chairman  
Department of Electrical and Computer Engineering

## ABSTRACT

In this research, continuing evidence that composite operational amplifiers perform better than single amplifiers in both gain bandwidth product and slewrate is presented through an approach of using computer simulation to predict ionizing radiation degradation. This technique examines the use of varying transistor parameters within PSPICE modeled composite and single operational amplifier circuits in order to simulate ionizing radiation. A comparison of the results of this simulation with those of previous research, in which composite and single operational amplifiers were irradiated with a LINAC, verifies that this simulation technique provides a reasonable prediction of a response to ionizing radiation for circuits comprised of radiation hardened components. And, in the process of validating this technique, these simulation results verify that composite operational amplifiers offer an improved bandwidth and a faster slewrate compared to single operational amplifiers.

## TABLE OF CONTENTS

I.	INTRODUCTION.....	1
II.	THE RADIATION ENVIRONMENT.....	6
III.	SEMICONDUCTOR DEVICES.....	17
IV.	TOTAL DOSE EFFECTS ON SEMICONDUCTOR DEVICES.....	26
V.	SINGLE AND COMPOSITE OPERATIONAL AMPLIFIERS.....	33
VI.	RADIATION EFFECTS ON OPERATIONAL AMPLIFIERS.....	43
VII.	SIMULATION PROCEDURE.....	48
VIII.	RESULTS.....	63
IX.	CONCLUSIONS AND RECOMMENDATIONS.....	76
	REFERENCES.....	78
	INITIAL DISTRIBUTION LIST.....	80

## **ACKNOWLEDGMENTS**

I must first thank my advisor, Dr. Sherif Michael, whose infinite patience, technical adroitness, and gentle supervision navigated me through the Naval Postgraduate School. I would like also to thank Dr. Hal Titus for his humor and generous counsel, and Colin Cooper and the Servo Controls Lab personnel for their support.

## I. INTRODUCTION

Over the last few decades we have seen an explosion in the advancement of electronics technology which has resulted in smaller, faster, and less expensive integrated circuits. Integrated circuits are the building blocks of today's high-tech systems for commercial, industrial, and defense applications. Our increased employment of space satellites and nuclear power, combined with shrinking circuit size, dictates the requirement for smaller, more-sensitive integrated circuits that will withstand tougher radiation environments. Without a solid understanding of the radiation environment, semiconductor physics, and the effect of radiation on semiconductor devices, our ability to operate systems which affect our daily lives, such as communications satellites, is degraded.

One method of protecting electronics from radiation is to thicken side panels or to add radiation shielding materials, such as individual shield housings, so that radiation penetration is decreased; another is to imbed the circuitry within other components to effect radiation shadowing. These options, however, may not always be possible or practical. For most systems, such as spacecraft, increasing panel thickness and adding individual shield housing results in a heavier, more costly bus. Additionally, other factors may carry more weight in driving a system's internal configuration than radiation protection. For example, in a geosynchronous three-axis stabilized spacecraft, the communications equipment is mounted on the north- and south-facing bus panels for

thermal isolation, ruling out the possibility of radiation shadowing. For these reasons, it is worthwhile to explore a third option of utilizing radiation resistant circuits.

Electronic circuits may be built from components which are radiation hardened (rad hard) in the manufacturing process. Alternatively, circuit components may be arranged into novel configurations, or have inherent characteristics, which increase a circuit's tolerance (rad tolerance) to radiation. These techniques are contrasted in Table 1 [Ref 1:p. 2.4-1], which was extracted from Harris Semiconductor's *Space Product News*. A commercial device is, as might be surmised, neither rad hard nor rad tolerant.

Rad hard components are guaranteed by the manufacturer to survive, i.e., remain within data sheet limits, when exposed to a given radiation level. Dielectric isolation, silicon on insulator (SOI) and silicon on sapphire (SOS) technology, and higher gate complexity are all examples of radiation hardness design techniques used by manufacturers [Ref. 2:p 3.1.1-2]. While rad hard techniques are the most reliable of the three, the complexity of the manufacturing process may prove rad hard components to be unaffordable for some applications, particularly in an era of budget constraints.

Rad tolerant devices, on the other hand, provide a less expensive alternative for protecting system circuits in a radiation environment. Rad tolerance techniques place less emphasis on component manufacturing processes, where rad hard costs are incurred, by employing components which are inherently less sensitive to radiation, or seeking innovative ways to rearrange the commercial components within existing circuits to minimize radiation sensitivity. Naturally, there is a trade-off: rad tolerant devices are



TABLE 1.1 GENERAL CHARACTERISTICS OF RAD HARD, RAD TOLERANT, AND COMMERCIAL INTEGRATED CIRCUITS

RAD HARD	RAD TOLERANT	COMMERCIAL
Designed for a specific hardness level	Hardness offered as a by-product of the design	Hardness limited by inherent process and design; customer risk
Wafer lot rad test	Sample rad test	Customer rad test
Guaranteed to remain within data sheet limits	Usually tested to functional fail only	Customer rad test and risk
Total Dose: >200 krad to >1Mrad	20 krad to 50 krad (typical)	2 krad to 10 krad (typical)
Latchup: <i>SOI techniques</i> : none <i>Bulk rad hard techniques</i> : guaranteed extremely low sensitivity	Customer evaluation and risk	Customer evaluation and risk

less reliable. In order to prove radiation tolerance of a proposed rad tolerant circuit, individual lot-to-lot testing could be required since no twin components are *precisely* the same. Minute manufacturing differences from component to component, which might even be transparent to the manufacturer, may lower radiation tolerance. In summary, rad tolerant devices are less expensive, albeit less reliable, than their rad hard counterparts.

The operational amplifier (op amp) may be considered to be the basic building block of a wide range of electronic circuits. An op amp is composed of numerous semiconductor devices which may be radiation hardened to collectively protect the op amp from radiation degradation. Incidentally, op amps composed of rad hard devices

inherently have large parameter fluctuations as a result of the rad hard manufacturing processes [Ref. 3:p. 3]. The response of op amps to radiation is determined experimentally for a single application when exposed to a particular amount of radiation. If the circuit is later modified, further testing and evaluation are required. In this thesis single op amp radiation response and the radiation response of a combination of op amps which replace a single amplifier, called a *composite operational amplifier*, are investigated and compared.

A composite op amp is an arrangement of two or more op amps which acts as a single op amp but with improved characteristics, of which one is an improvement in radiation sensitivity. While combining single op amps together to form a composite op amp will not increase radiation hardening of the single op amp circuit, they are expected to decrease overall active circuit sensitivity to radiation.

Composite op amps may be physically realized using Bipolar Junction Transistors (BJTs), Field-Effect Transistors (FETs), or Metal-Oxide Semiconductor Field-Effect Transistors (MOSFETs or MOS). Both Bipolar Junction op amps and Complimentary MOSFET (CMOS) op amps were included in this research, which simulates and compares the radiation response of single and of composite operational amplifiers. BJT components, which are popular due to their fast response and high gains, were chosen to allow comparison between the simulation results of radiation models and previous experimental results obtained by actually irradiating BJT op amps using a linear accelerator [Ref 11].

CMOS op amps, on the other hand, are popular due to their small size, high input impedance, easy construction, and low power consumption. The drawback to CMOS devices in general is due to their higher sensitivity to small amounts of ionizing radiation. A hybrid circuit utilizing a combination of BJT and CMOS (BIMOS) devices which is subject to ionizing radiation will have a degradation response dominated by the more sensitive CMOS devices. For this reason, it was important to include CMOS devices in the simulation.

In this research, single and composite BJT and CMOS op amps were modeled in a finite amplifier configuration using the PSPICE circuit simulation program. Total dose radiation effects were then simulated by modifying device parameters within the op amp. The outputs of both composite and single op amps were then compared using MATLAB to process and plot the extracted data from the PSPICE output.

Chapter II explores natural and man-made radiation environments.

Chapter III reviews basic semiconductor physics.

Chapter IV examines radiation effects on semiconductors.

Chapter V reviews op amp operation and composite op amp theory.

Chapter VI considers radiation effects on single and composite op amps.

Chapter VII presents the models used and steps taken in the simulation.

Chapter VIII analyzes and displays graphs of the simulation results.

Chapter IX offers recommendations and conclusions.

## II. THE RADIATION ENVIRONMENT

Radiation may be traced to either man-made sources or natural sources. Natural sources of radiation consist of the sun and galactic cosmic rays, while man-made sources of radiation of interest are nuclear reactors and nuclear weapons, all of which are characterized in Table 2.1 [Ref 12:p. 4]. Although they are quite different, it is conceivable to have both sources of radiation in the same environment: the systems

TABLE 2.1 SUMMARY OF MAJOR RADIATION DAMAGE AREAS

Application	Damage Effect	Radiation*	Device Affected
Nuclear weapons	Displacement	$n$ only	Bipolar transistors
	Ionization	Transient	All semiconductor devices
		Surface	IGFETs
Nuclear reactor	Displacement	$n$ and $\gamma$	Bipolar transistors
	Ionization	Transient	No problem
		Surface	Bipolar transistors and IGFETs
Van Allen Belts	Displacement	$e$ and $p$	Solar cells only
	Ionization	Transient	No problem
		Surface	Bipolar transistors and IGFETs

\* $n$  — neutrons       $\gamma$  — gamma rays  
 $e$  — electrons       $p$  — protons

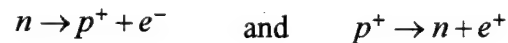
engineer of a nuclear powered spacecraft would have to consider both sources of radiation when configuring equipment panels and selecting power subsystem components. For this reason, it is necessary to understand both radiation sources and the environments they create in order to predict, and ultimately protect against, their effects on semiconductors. In this chapter, radiation-related particles and processes are first catalogued in order to facilitate the ensuing description of both natural and man-made environments.

## **A. RADIATION-RELATED PARTICLES AND PROCESSES**

### **1. Charged Particles**

Charged particles include electrons, protons, beta particles, and alpha particles.

Beta particles are "fast electrons" emitted from decaying nuclei in the form



and so they may be further defined as being comprised of electrons and positrons, also known as "antielectrons" or "positive electrons." Alpha particles, which are comprised of helium nuclei (2 protons and 2 neutrons), are much larger in size and are extremely heavy compared to beta particles. They are the result of nuclear fusion reactions. Both alpha particles and beta particles have a short range in media, such as air, due to charge interactions. This is particularly true for the relatively sluggish alpha particles. A sheet of aluminum, such as a satellite panel, or even the next collective fifty pages of this thesis effectively shield most alpha particles. [Ref 6:p. 143]

## 2. Photons

Photons are small packets of electromagnetic energy which travel at the speed of light, are mass-less, and are uncharged. There are two types of photons of primary interest: X-rays and the higher-energy gamma rays. Both are products of nuclear fission. X-rays are emitted when high-energy charged particles incident on or through a medium lose kinetic energy. Gamma rays, which are highly penetrating, are emitted from nuclei as a result of either radioactive decay or the release of energy after nuclear absorption of a neutron (neutron capture). Photons are responsible for the following three ionizing reactions:

### *a. Photoelectric Effect*

When a relatively low-energy X-ray passes near the nucleus of an atom, it excites the atom causing it to shed an innermost electron, thereby ionizing the atom but losing all of its energy in the process. The replacement of the lost electron by a second electron in a higher shell causes the emission of a photon, as does the subsequent replacement of the second electron by a third in an even higher shell, etc., known as the *photoelectric effect*.

### *b. Compton Effect*

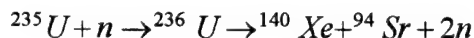
The *Compton effect* involves the collision of a relatively high-energy X-ray with an electron, resulting in ionization and only a loss of a portion of the photon's energy (or lowered frequency) instead of annihilation. This then permits the X-ray, and the free electron, to ionize other atoms until eventually coming to rest.

### ***c. Pair Production***

In *pair production*, very high-energy photons, or gamma rays, are annihilated when passing near an atomic nucleus, creating an electron and a positron which are each capable of ionizing other atoms.

### **3. Neutrons**

Neutrons are generated by both nuclear fission, which is the splitting of a single element into multiple elements, and nuclear fusion, which is the reverse of fission, and which occurs inside the Sun, stars, and thermonuclear reactions. Both reactions release energy. An example of both fusion and fission is the fusion of a neutron and a  $^{235}\text{U}$  nucleus to form  $^{236}\text{U}$ , which undergoes fission to produce fission fragments and two prompt neutrons: [Ref. 18:p.1104]



### **4. Ionization**

Ionization damage is the stripping of outermost shell electrons of an atom by an incident charged particle. In semiconductors, it results in the creation of free hole-electron pairs, such as in the three photon interactions previously discussed. Neutrons, which are heavy and uncharged, are incapable of *directly* causing ionization; however, they may induce the creation of other ionizing particles, for example, neutron capture by a nucleus after which an ionizing gamma ray is created. Instead, neutrons are renown for displacing entire atoms from their lattice structures. This is classified as displacement damage, and will be discussed later.

***a. Ionizing Dose Rate***

Ionizing dose rate is the rate at which ionization is accumulated as a result of the deposition of charged particles and photons on semiconductor material.

***b. Total Dose***

Total Dose is simply the integral of dose rate: it is the accumulation of ionization a circuit receives, measured in units of rads of silicon (rads(Si)), from the absorption of charged particles and photons in the semiconductor material. One rad is one hole-electron pair created per centimeter squared of irradiated material.

**5. Displacement**

As discussed earlier, displacement damage is caused by the displacement, or dislodging, of an atom from its lattice structure by relatively heavy particles. Most of the damage to electronic devices in this environment is attributed to neutron irradiation. Here, the relatively heavy neutrons bombard atoms within the semiconductor crystal, knocking them out of their stable positions. These displaced atoms may either take up interstitial positions or they may knock other atoms from their positions causing ionization and, ultimately, permanent defects within the material [Ref. 3:p. 161-2].

***a. Neutron Fluence***

Neutron fluence is the rate at which neutrons are incident upon a material. Neutron fluence is measured in neutrons incident per centimeter squared of irradiated material ( $N/cm^2$ ).



## **6. Single Event Upset (SEU)**

Single event upset is the upset of circuit elements due to a single particle strike from a heavy ion, such as an alpha particle. It is caused by the deposition of charge within a critical node resulting in a change-of-state, such as changing a memory cell or a logic circuit output from a 0 to a 1 state, or vice versa. As inferred, it is a serious problem for digital circuits. SEU upset is not included in this thesis for two reasons: the first is that SEU is caused principally by heavy ions from cosmic rays, and is not a major threat in orbits lower than geosynchronous since the earth's magnetic field deflects a majority of these ions. The second is that SEU poses a threat to digital circuits whereas the circuit elements and the proposed technique in this research are designed for analog circuits.

## **7. Annealing**

Annealing is the ability of a semiconductor to recrystallize ("heal" itself) in the presence of heat or current *after* having experienced radiation-induced defects. Because the space radiation environment is a continuous process, i.e., radiation from all sources is fairly constant, irradiated devices really do not have the opportunity to anneal. Annealing is more useful in the context of a pulse of radiation, such as a nuclear explosion, after which an irradiated device has a "rest" period during which it may anneal.

## B. NATURAL RADIATION

Natural radiation exists in interplanetary and planetary space. Interplanetary radiation, away from the influence of the earth's planetary magnetic field, is caused to a small degree by galactic cosmic rays which are protons and electrons from stars, and heavy ions from sources such as novas and supernovas. Its biggest contributor is the solar wind. The solar wind is a radial stream of mainly protons and electrons emitted during nuclear fusion within the Sun's interior whose intensity varies with solar flare and sun spot intensity [Ref. 4:pp. 2.2.1-2].

Solar flares occur randomly, emitting protons and a few alpha particles sparsely sprinkled with even heavier ions. Radiation from a solar flare reaches the earth within a few hours, peaks, then dissipates within a week. The solar wind, however, delivers residual solar flare radiation within a few days after a flare through striking and compressing the Earth's magnetosphere, increasing the radiation dose at lower altitudes above the earth. [Ref. 5:p. II-8].

In the Earth's planetary space, interplanetary charged particles are attracted by the Earth's magnetic field. Those particles that are below a critical energy will become trapped and gyrate around the Earth's magnetic lines of force, reflecting between mirror points as depicted in Figure 2.1 [Ref. 18:p. 695]. Collectively, these charged particles form bands which constitute the Earth's Van Allen belts. Figure 2.2 [Ref. 4:p. 2.2-4], which is an extract from Harris Semiconductor manuals, gives a rough estimate of the radiation exposure rates encountered by spacecraft with the following description:

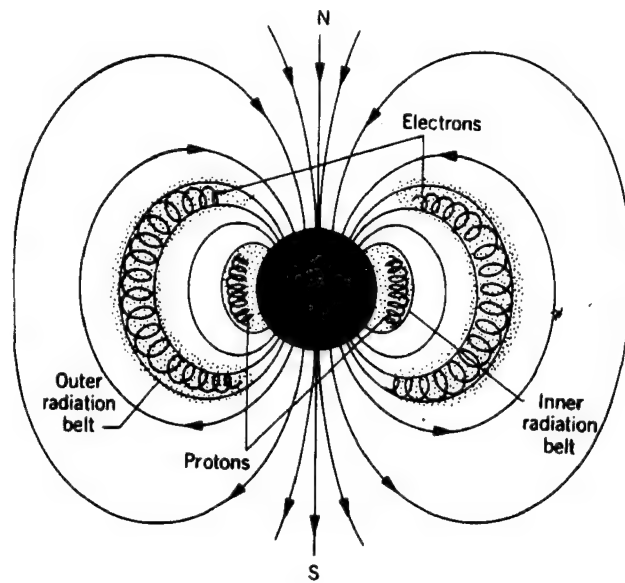


Figure 2.1 The Earth's Magnetic Field

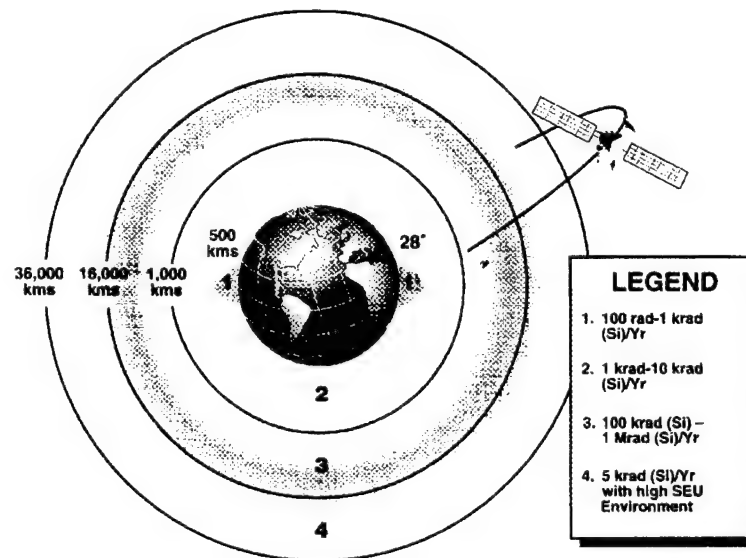


Figure 2.2 The Spacecraft Radiation Environment

1. The most benign environment is encountered by satellites in low inclination, low earth orbits (LEO) shown in area 1.
2. However, low earth orbits in a higher polar inclination encounter significantly increased dose rates due to the Van Allen belts dipping to low altitudes and a much higher heavy-ion flux due to the lack of magnetic deflection of the ions at the poles, as in area 2.
3. In area 3, the highest dose rates of up to 1 Mega rad per year are encountered. This area is attributed to being the densest region of the Van Allen belts.
4. Spacecraft in a geosynchronous orbit of  $0^\circ$  inclination and 35800 km altitude are on the fringe of the Van Allen belts and experience less ionizing radiation; however, at this altitude, the magnetic field is no longer strong enough to act as a shield against heavy ions, so the heavy ion flux increases. [Ref. 4:p2.2-4]

### **C. MAN-MADE RADIATION**

Unnatural or man-made radiation refers to nuclear radiation resulting from either nuclear powered systems or from nuclear weapons. Radiation from nuclear weapons or nuclear explosions is the "worst-case" in that it is characterized by infinite dose rates and/or total dose, it is extremely time-varying, and involves, either directly or indirectly, photons, neutrons, and charged particles. For illustrative purposes, the following section will discuss the variety of particles which result from a nuclear explosion.

Nuclear radiation is released both at the instant of the detonation and over an extended period of time. Radiation is the result of both fission and fusion reactions within the nuclear device and is released both at the instant of the detonation and over an extended period of time. Initial radiation consists of neutrons, photons, and alpha and beta particles, which in turn cause secondary radiation through ionization or the release

of energy after capture. Neutrons are generated by both fission and fusion detonation reactions and are principally responsible for producing radioactive materials within and without the explosion confines. Neutrons travel with a velocity that depends on their energy and interact with material to produce additional gamma rays. In this manner, neutrons are responsible either directly or indirectly for ionization and displacement damage. [Ref 3:pp. 142-3]

Most of the energy of an explosion is emitted as X-rays, which are the principal agent that ionizes the air to create what is known as a fireball. X-rays are readily absorbed by the intervening matter. Gamma rays, on the other hand, are very fast and highly penetrating, traveling at the speed of light regardless of their energy. Both initial and neutron-induced gamma rays cause ionization. [Ref 3:pp. 142-3]

Alpha and beta particles, as discussed earlier in this chapter, are the result of fusion reactions and decaying nuclei, respectively. Due to their short range, they are not considered to be major contributors to radiation in this scenario. [Ref. 3:pp. 142-143]

#### **D. THESIS RADIATION ENVIRONMENT**

For spacecraft in a geosynchronous orbit and below, ionizing radiation trapped within the earth's magnetic field poses the greatest threat to electronics. In the natural space environment, dose rates are typically low (measured in rads(Si) per year) and are continuous compared to other radiation sources, such as nuclear explosions, where a burst or pulse of radiation is experienced. Radiation incident on a spacecraft is measured in terms of accumulated dose at the end of the spacecraft's life (EOL). Spacecraft are

designed to meet mission requirements throughout a lifetime total dose of radiation. For these reasons, total dose degradation due to ionizing radiation (total dose) and its effects on semiconductor devices are simulated and are the main subject of research in this thesis.

### **III. SEMICONDUCTOR DEVICES**

There are two major types of semiconductor devices: the Bipolar Junction Transistor (BJT) and the Field-Effect Transistor (FET). The majority of analog circuits are designed using BJTs due to their high gain-bandwidth product. On the other hand, the use of FETs is minimal in analog applications because of its relatively small gain-bandwidth product, which restricts its use to digital circuits. However, the FET offers high input impedance, easy construction, and low power consumption. Therefore, it is very important in the design of very large scale integrated circuits (VLSI) since it may be made quite small in size, thus occupying less silicon real estate on an Integrated Circuit (IC) chip. This chapter first discusses the BJT, then a special FET circuit called the Complimentary Metal on Oxide Semiconductor (CMOS) FET.

#### **A. BIPOLAR JUNCTION TRANSISTORS**

Within the BJT there are three semiconductor regions: the emitter, the base, and the collector. Each region consists of either n-type or p-type material. N-type material is a semiconductor doped with atoms that can donate an extra electron, thus produces negative carriers. On the other hand, p-type material is a semiconductor doped with atoms that can accept an extra electron which creates a positively charged "hole," thus produces positive carriers. For an npn transistor, both the emitter and the collector are made of n-type material and the base is made of p-type material; in a pnp transistor, the reverse is true. Hence, the npn and pnp BJT may be respectively modeled as either two

back-to-back or two front-to-front diodes. To avoid repetition in the ensuing discussion of active transistor operation, only the discussion of an npn transistor will be considered, since a pnp transistor functions similarly except the current is reversed.

A transistor is biased to operate in the active linear mode if it is to operate as an amplifier. An example of an npn transistor biased as such is shown in Figure 3.1 [Ref. 5:p. 194], where current flow in the outside circuit represents the flow of positive charge (holes). Additionally, Figure 3.2 [Ref. 5:p. 200] illustrates an npn BJT cross section.

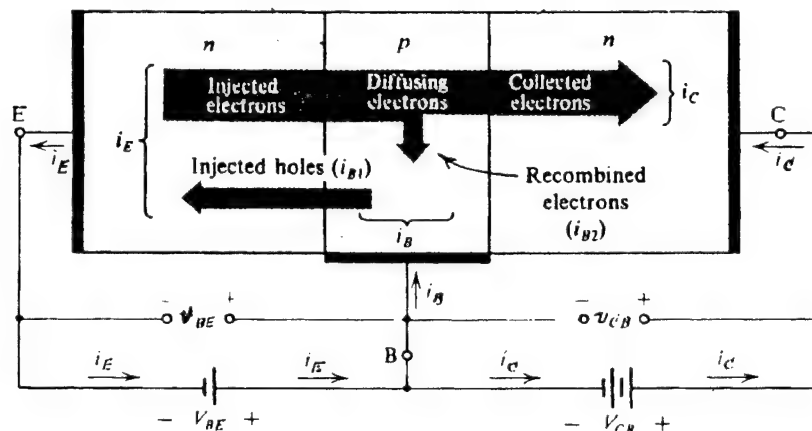


Figure 3.1 An NPN Transistor

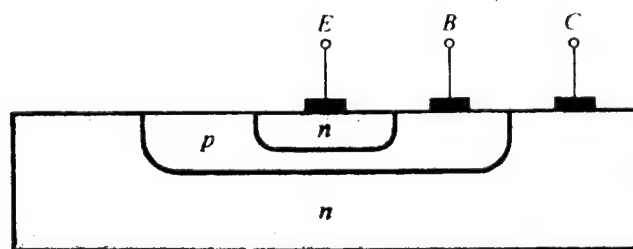


Figure 3.2 An NPN BJT Cross-Section



## **1. Emitter Current**

Referring to Figure 3.1, the voltage  $V_{BE}$  causes the p-type base to be higher in potential than the n-type emitter, which forward biases the base-emitter junction. This causes a current to flow in the emitter which in turn is the sum of two components: holes transiting from the base to the emitter, and electrons transiting from the emitter into the base. Due to a higher doping of n-type material in the emitter than p-type material in the base, the hole component is very small compared to the emitter component, so that the emitter current refers only to the electrons transiting from the emitter to the base. These electrons are called "minority carriers," since they become minorities in the p-type base region. [Ref 5:pp. 194-195]

## **2. Base Current**

Once inside the base, it is logical to assume the minority carriers recombine with the majority carriers within the base. The number of minority carriers that recombine is proportional to the doping level of the p-type base material and inversely proportional to the width of the base. In actuality, very few of the minority carriers recombine. There are two reasons for this. The first, which was alluded to earlier, is that the differences in doping between the emitter and the base lead to a much higher population of electrons than holes in the vicinity. Of equal importance, the width of the base is purposefully very thin. So the cumulative result is that most of the minority carriers that transit to the base are able to continue on to the collector-base depletion region. [Ref 5:pp. 194-195]

### 3. Collector Current

Because the collector is biased at a higher potential than the base, i.e.,  $V_{CB}$  is positive (reverse biased), those minority carriers residing in the base-collector depletion region are swept into the collector as collector current.

In addition to the above-mentioned minority carriers, an additional parameter which will be important in future discussions of radiation effects is reverse currents. Thermally generated minority carriers produce reverse currents, which are usually small. However, reverse currents in the collector-base junction are actually much higher than predicted, and are dependent on both  $V_{CB}$  and temperature. [Ref 5:pp. 194-195]

### 4. Common Emitter Current Gain

Perhaps the most important transistor parameter is the common emitter current gain, denoted by  $\beta$ . While  $\beta$  varies from transistor to transistor, it usually ranges between 100-200 for npn transistors and a little less for pnp type.  $\beta$  is the ratio of collector current to base current,  $\beta = I_C/I_B$  and, as such, is highly dependent on the relative doping levels of the collector with respect to the base, as well as on the base width. Since  $\beta$  represents current gain, it is desired and designed to be of high value, which in retrospect explains why the base is thin and lightly doped in comparison to both the collector and emitter [Ref 5:pp. 196-197].

## B. MOSFET (MOS) TRANSISTORS

The Field Effect Transistor (FET) is also referred to as a *unipolar* transistor since current flow is due only to the motion of majority carriers in contrast to BJTs, whose

operation depends on minority carrier flow in the transistor base region. FETs also differ from BJTs in that current flow is parallel to the surface, whereas in a BJT it is mainly perpendicular. [Ref 12:p.141]

As the name implies, a Metal Oxide Semiconductor (MOS) transistor has an oxide layer inserted to insulate the metallic base-like terminal, or gate, from the semiconducting material. It is this insulation which causes the current in the gate terminal to be extremely small and, hence, allows the overall size of the device to be small [Ref 5. p. 301]. Additionally, MOS devices are simple to construct, so that large numbers of devices may be produced for a low cost, and MOS devices are also known for their low power consumption. A CMOS transistor is composed of two MOS transistors: one which consists of an n-channel imbedded in a p-type material, called an NMOS transistor, while the other is a p-channel imbedded in an n-type material, called a PMOS transistor. Below is a description of NMOS operation. A PMOS transistor performs similarly to an NMOS, only the current flow is reversed.

### **1. NMOS Transistor Operation**

There are three terminals within an NMOS transistor: the source, the gate and the drain. Figure 3.3 [Ref. 5:p. 300] provides a physical schematic of an NMOS transistor. According to Sedra and Smith [Ref. 5], the following discussion of NMOS operation is divided into phases which are a function of the magnitude of the voltage from gate to source,  $v_{GS}$ , and from drain to source,  $v_{DS}$ .

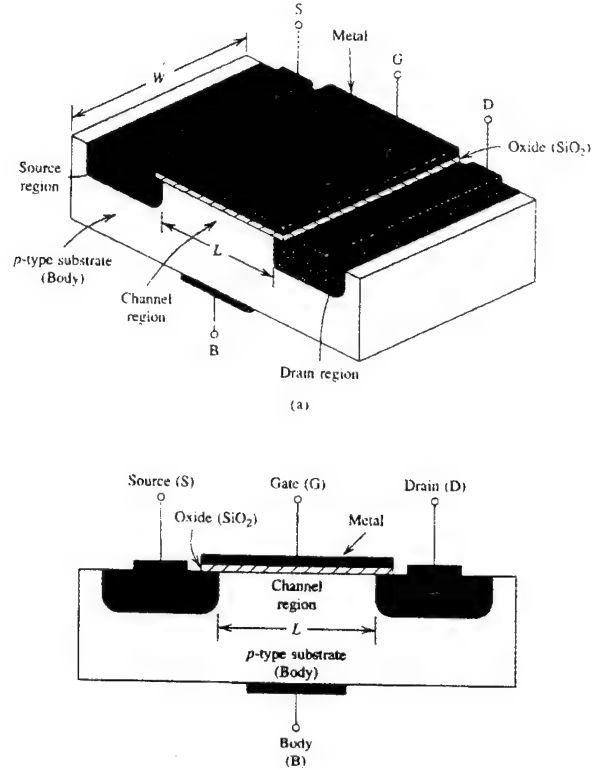


Figure 3.3 An NMOS Transistor

**a. Operation Without a Gate Voltage**

With no voltage applied to the gate,  $v_{GS}$ , two back-to-back diodes exist between the drain and the gate terminals which will not conduct current in the presence of a potential applied between drain and source,  $v_{DS}$ .

**b. Operation With a Small Drain Voltage**

With the source grounded and a small positive voltage applied to the gate,  $v_{GS}$ , holes in the vicinity of the gate are repelled from the positive gate bias, while electrons are attracted and fill in the depletion region left by the holes. If the gate voltage

$v_{GS}$  is of a sufficient magnitude, enough electrons accumulate near the gate to form a passage between drain and source, thereby creating a channel for current to flow. The minimum required  $v_{GS}$  to induce current flow is called the *threshold voltage*, denoted by  $V_t$ .  $V_t$  is typically within the range of 1 to 3 volts. The amount of current that flows for a given  $v_{DS}$  is controlled by the magnitude of  $v_{GS}$ . Hence, the greater  $v_{GS}$  is, the more electrons that will be attracted into the channel, and the greater the channel depth. [Ref 5:pp. 301-2]

### c. Operation With a Large Drain Voltage

For a given  $v_{GS}$  or channel depth, an increase in  $v_{DS}$  up to a saturation voltage of  $v_{DS} = v_{GS} - V_t$  results in a linear increase in the current flowing through the channel as depicted in Figure 3.4 [Ref. 5:p. 305]; however, at the same time, the channel

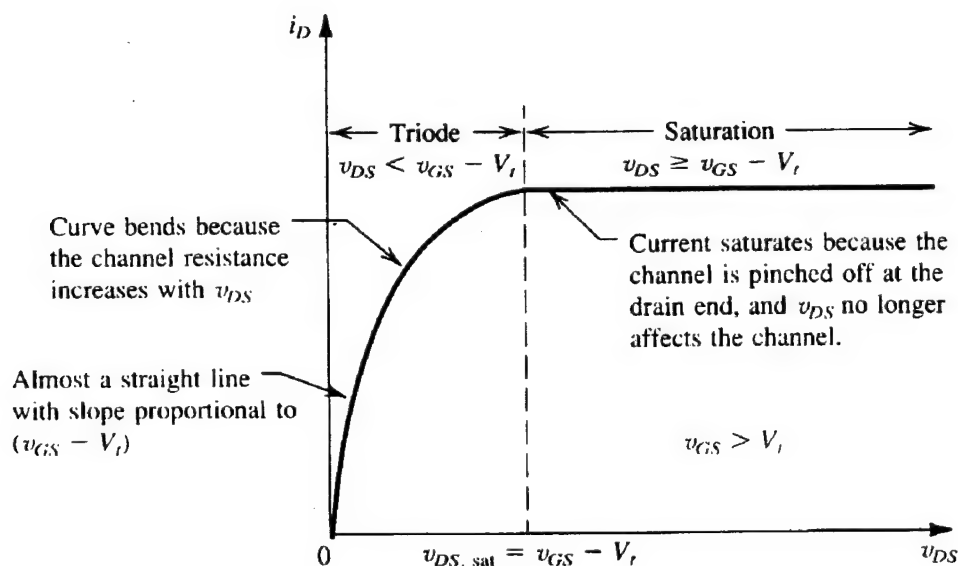


Figure 3.4 NMOS Current

becomes more tapered at the drain end. This tapering is due to the fact that  $v_{DS}$  appears along the length of the channel, varying from  $V=0$  at the source end to  $V=v_{DS}$  at the drain end. Once  $v_{DS}$  reaches the saturation voltage, the drain end is pinched off and the transistor is said to have entered the pinch-off region, where  $v_{DS}$  no longer affects current flow. [Ref. 5:pp. 305-306]

## 2. CMOS Operation

CMOS circuits are the most useful of all the analog and digital integrated circuit MOS technologies. A CMOS cross-section is illustrated in Figure 3.5 [Ref. 5:p. 307]. Note that while the PMOS transistor utilizes the n-type body, the NMOS draws on a well of p-type material, and that the two are insulated by a thick region of oxide. By

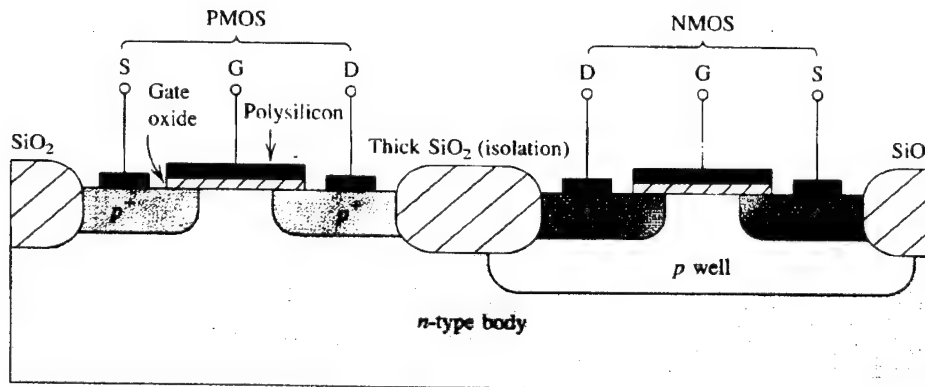


Figure 3.5 CMOS Cross-Section

providing both transistor types, CMOS transistors allow much greater flexibility in circuit design compared to NMOS, and the resulting circuits exhibit improved performance over those fabricated with NMOS technology [Ref 5:p. A-10].

## IV. TOTAL DOSE EFFECTS ON SEMICONDUCTORS

### A. DEGRADATION IN BIPOLAR JUNCTION TRANSISTORS

While new BJT devices have become less sensitive to displacement damage over the past ten years, total dose-induced gain degradation is still a major concern for bipolar transistors [Ref 14:pp. III-19-20]. This is particularly true if BJT devices are to operate in high-gain, low-current applications, such as in operational amplifiers.

Degradation of the current gain parameter,  $\beta$ , is the primary effect of ionizing radiation incident on bipolar transistors. Ionizing radiation penetrates and affects both the oxide layer and the substrate beneath it. In the oxide layer, incident radiation creates inversion layers (positive charge on an n-substrate surface and negative charge on a p-substrate surface) along the exposed transistor surface due to trapped ionization-induced charge. These inversion layers increase generation-recombination currents and create space charge regions along the oxide layer. This phenomenon predominantly affects the more-sensitive base region due to its relatively thin width and low doping level. The overall base current is the total of the current drawn into the base-collector depletion region plus the current drawn into the inversion layer depletion region. In spite of increasing base current and shifts in the collector-base space charge region, the much larger collector current ( $I_C = \beta I_B$ ) is impervious to these relatively small changes. Increased base current for a fixed collector current reduces the bipolar transistor current gain parameter as  $\beta = I_C / I_B$ , and, incidentally, affects the transistor most



when the transistor has a high gain and is operated at low current. This is primarily due to the fact that low current levels are surface currents, and are thus affected by the inversion layers discussed earlier. Figure 4.1 [Ref. 3:p. 257] depicts the relative gain degradation as a function of ionizing dose level for 43 different transistor types.

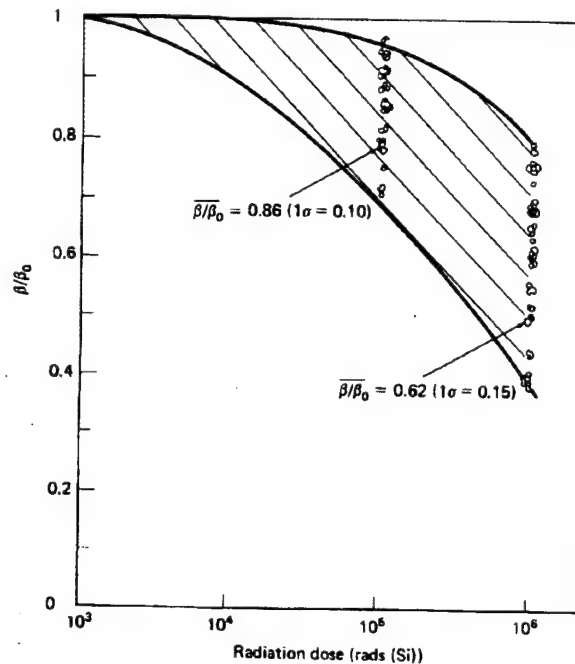


Figure 4.1 Relative Gain Degradation as a Function of Ionizing Radiation for 43 Different Transistor Types

While these effects are precipitating from radiation incident on the oxide layer, ionizing particles which weave their way past the oxide layer are able to shoot into the substrate, creating electron-hole pairs along their paths. From these pairs, the highly mobile electrons contribute to the minority carrier current in the base. Through recombination, the increased base current shifts the base-collector space charge region

further into the collector, increasing the base width. In turn, the increased base width results in an increase in base transit time and so reduces the gain bandwidth product  $f_t$ .

[Ref. 3:pp. 254-258]

The amount of base current generated from radiation-induced inversion layers varies greatly due to the manufacturing process of each family of semiconductor device, which changes the device structure and impurities within the silicon dioxide layer. A particular semiconductor's response to radiation also depends on the bias condition under irradiation: NPN transistors show greater gain degradation when biased, while PNP show greater gain degradation when they are unbiased. Due to all of these uncertainties, a specific correlation between  $\beta$  and total dose is unknown. An excerpt from Messenger [Ref. 3:pp. 255-256] serves to legitimize and reiterate the above:

Because ionization damage ultimately results in complex surface effects, and because device structures are topologically very diverse, there is at present no theoretically rooted gain degradation expression as a function of ionizing radiation fluence or absorbed dose, as there is for bipolar gain degradation due to neutron fluence.

In the absence of equations, there are some general guidelines for associating  $\beta$  with total dose which may be gleaned from a few references. From Messenger and Measel, [Ref 3 and Ref 14], a reduction in  $\beta$  of 50% results from an irradiation that ranges between .2 and 10M rads(Si). Figure 4.2 is an extrapolation of data from Figure 4.1, and associates a reduction in  $\beta$  of 90% to a total dose of between 3M-50M rads(Si), and reductions in  $\beta$  of 95%, 96%, 97%, and 97.5% to total doses of 7M-70M, 7.5M-80M, 8M-90M, and 8.5M-100M rads(Si), respectively. Referring to Figure 2.1, 10M rads(Si)

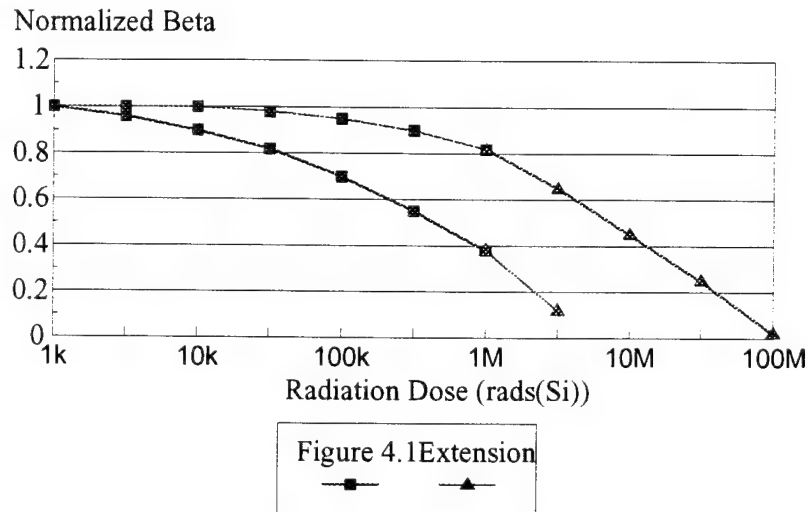


Figure 4.2 Extension of Figure 4.1

is approximately equal to the amount of radiation a spacecraft experiences at the end of a ten-year life, while orbiting the densest region of the Van Allen Belts, which is at an altitude of 16,000 kms. An example of such spacecraft is the Global Positioning System (GPS) satellites which orbit the Earth at approximately this altitude.

With all of this in mind, it is important to emphasize that BJTs are much more tolerant to ionizing radiation than are CMOS devices. Since the BJT is characterized by small base widths to effect high efficiency and perpendicular current flow, the above-mentioned surface effects are not as devastating to BJTs as they are to CMOS devices, which depend on surface interactions for their operation.

## B. DEGRADATION IN MOS TRANSISTORS

Shifts in MOS transistor threshold voltages due to silicon/silicon dioxide interface charge trapping is the dominant mechanism causing device degradation. Figure 4.3 [Ref.

4:p. 2.3-2] shows a schematic representation of the generation and trapping of positive charge (holes) within the oxide layer of a MOS transistor. Figure 4.3A shows the preirradiation MOS oxide layer cross section, while Figure 4.3B is the immediately post-irradiation case. Figure 4.3C shows a reduction in electron-hole pairs due to recombination, where, if there were no gate bias, all of the pairs would recombine. Figure 4.3D shows the mobile electrons migrating to the positively biased gate while the

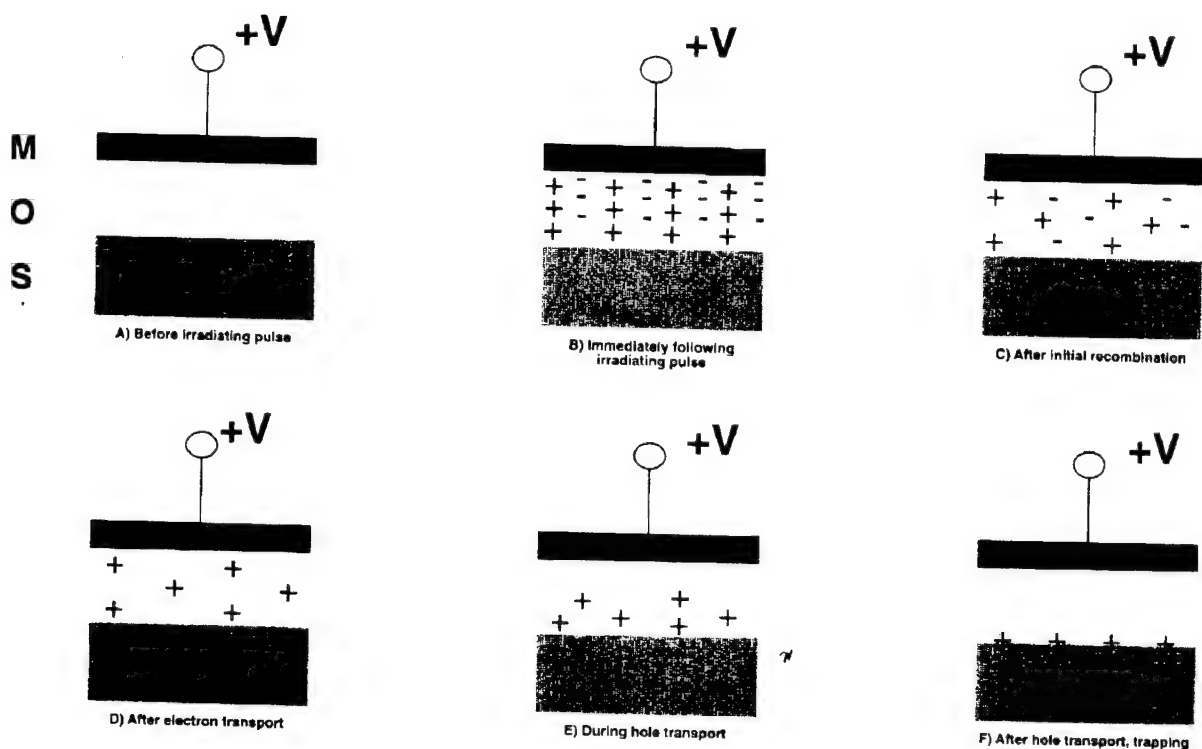


Figure 4.3 Generation and Trapping of Charge in an NMOS Transistor

much slower holes migrate away from the gate and towards the channel as depicted in Figure 4.3E. Figure 4.3F shows hole trapping at the interface, which is dependent on interface quality, oxide purity, and several other factors. These trapped charges cause transistor thresholds to decrease, such that N-channel transistors become easier to turn on, and P-channel transistors become harder to turn on.

Another phenomenon which occurs in MOS transistors at high accumulated doses is interface states. Interface states are generated by mechanisms which are only partly understood, and are highly dependent on fabrication techniques. Their overall effect, as depicted in Figure 4.4 [Ref. 4:p. 2.3-3], is to increase N-channel transistor threshold voltages, leaving P-channel thresholds untouched. Figure 4.4 shows charge buildup and interface state effects on threshold voltage versus total dose for both N- and P-channel

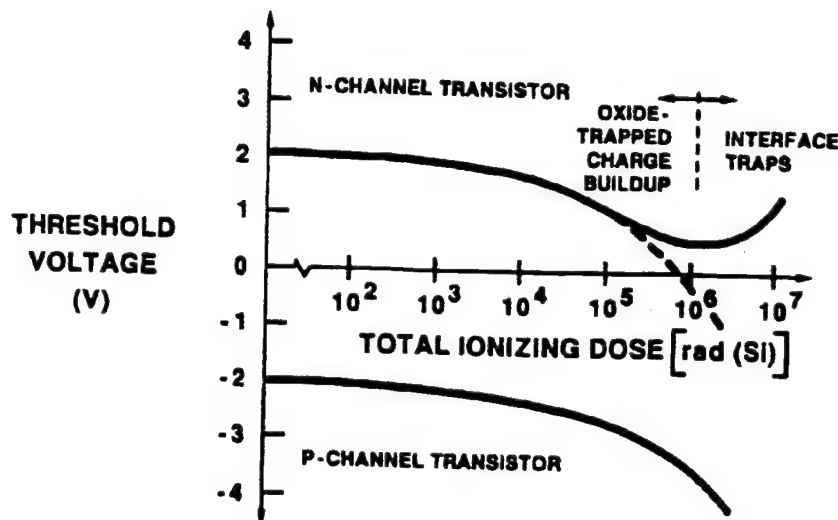


Figure 4.4 Charge Trapping Effects on MOS Threshold Voltages

MOS transistors. Due to the varying effect between P- and N-channel transistors, CMOS devices, which utilize both types, have complex failure modes which are difficult to predict. For these reasons, changes to CMOS threshold voltages due to interface traps would be very difficult to analyze, and so were not simulated in research of this thesis.

[Ref. 16:p. 1512]

## V. SINGLE AND COMPOSITE OPERATIONAL AMPLIFIERS

An operational amplifier (op amp) is probably the most widely used analog circuit building block due to its versatility and nearly ideal characteristics, which make circuits utilizing op-amps easy to design. There are generally three types of op amps: bipolar, CMOS, and a combination of the two termed BiCMOS. Bipolar op amps perform better in analog circuits, while CMOS op amps perform better in digital circuits.

Made up of a large number of transistors and resistors and a single stabilizing compensating capacitor, the op amp is a complex circuit whose performance is driven by the current gain within each transistor ( $\beta$ ). Figure 5.1 [Ref 5:p.700] illustrates a 741 internally compensated op amp -- one of the most popular op amps today, which is currently produced by almost every manufacturer of analog semiconductors. As such, the 741 op amp is the type of bipolar op amp used in this simulation.

### A. OP AMP THEORY

Driven by transistor current gain, op amp performance may be measured in terms of three parameters which will be discussed in turn: 3dB frequency, gain, and slew rate. The *3dB frequency*, or half-power point, is important in that it is a measure of the full operational bandwidth of the op amp. The 3dB frequency is, in turn, determined by the dominant pole introduced by the op amp's single capacitor.

Op amp gain is given by the transfer function  $A = A_o \omega_L / (\omega_L + s)$ , where  $A_o$  is the DC gain, and  $\omega_L$  is the 3dB frequency. As a reminder,  $\omega_L$  is the frequency in radians per second, and  $f_L$

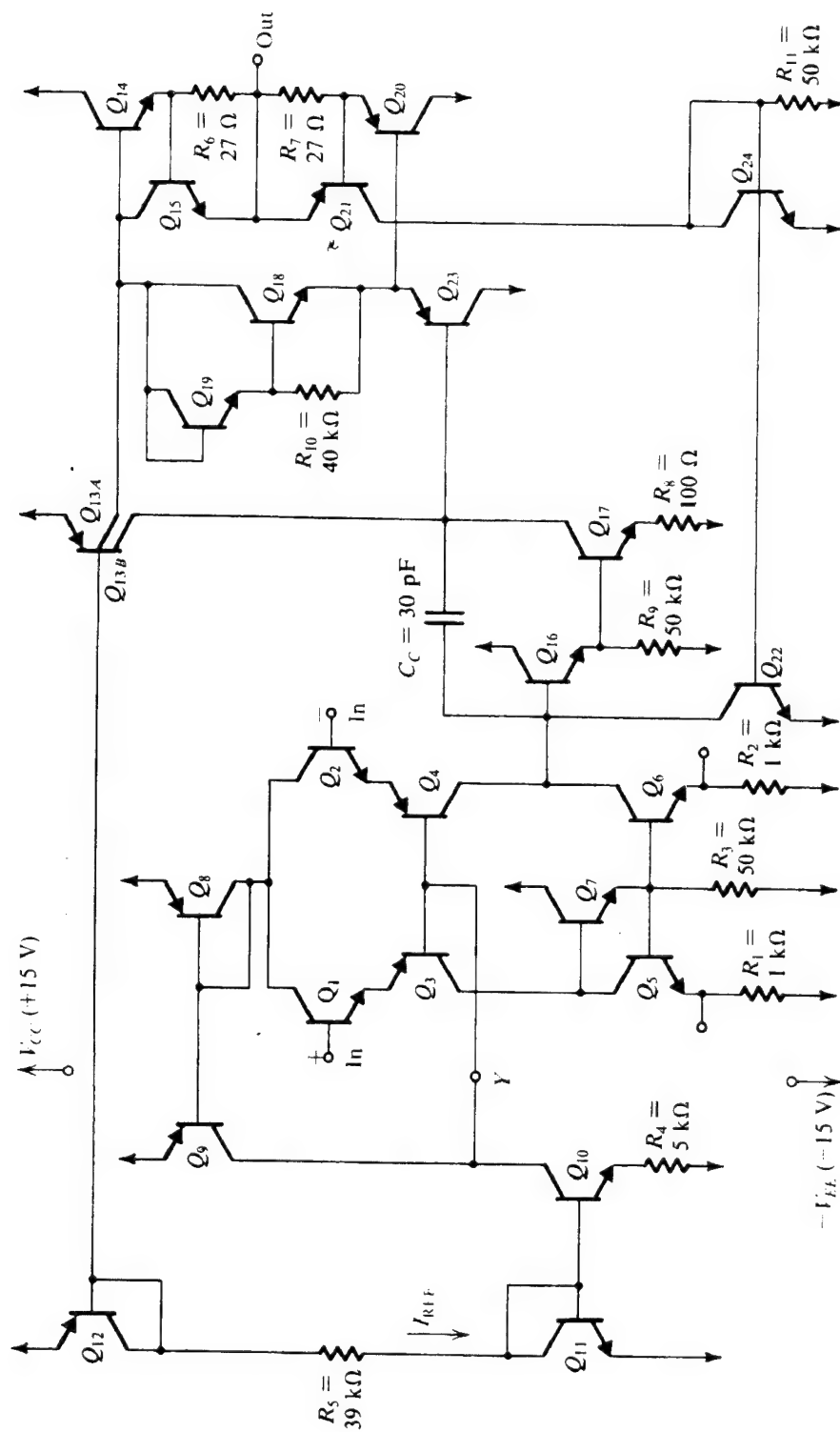


Figure 5.1 741 Op Amp



is the frequency in cycles per second (Hz). For frequencies  $\gg \omega_L$ , the gain reduces to  $A = A_o \omega_L / s$ . Another parameter is the gain bandwidth product ( $f_t$ ). The  $f_t$  is given by  $f_t = A_o f_L$ , which is a constant for any operational amplifier and is often used as a figure-of-merit. Figure 5.2 [Ref. 5:p. 724] illustrates  $A_o$ , 3dB frequency, and  $f_t$ .

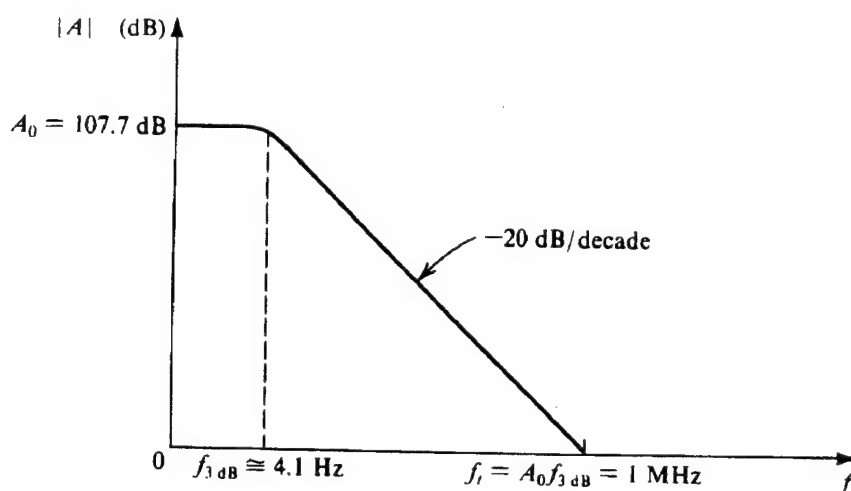


Figure 5.2 Ideal Op Amp Frequency Response

The *slew rate* is the maximum possible rate-of-change of the op amp output voltage. The slew rate depicts the ability of the op amp output to follow a time-varying input. The slew rate of a compensated op amp is driven by the time needed to charge or discharge the internal compensating capacitor. Therefore, the slew rate is relative to the size of this capacitor, which is needed to introduce the dominant pole in the op amp transfer function for stable operation. The expected time response, considering only the dominant pole, is a single-time constant response given by

$$V_{out}(t) = V_{in}(1 - e^{-t/\tau})$$

In practice, such a response is only obtained for small (less than 1V<sub>peak</sub>) inputs. For larger inputs, slew rate limiting may turn a sine wave into a triangular wave thus introducing nonlinear distortion. The maximum slew rate of an op amp is given by  $SR = I_{max}/C$ , and, hence, is a function of the maximum current through the capacitor in the second stage and the magnitude of the capacitance, which is typically small to effect fast slew rates. Op amp slew rate is determined by  $SR = [dV_o/dt]_{max}$ , and is usually expressed in V/s.

## **B. COMPOSITE OP AMP THEORY**

In an effort to extend the operational bandwidth and improve the performance of operational amplifier circuits, Wasfy B. Mikhael and Sherif Michael developed composite operational amplifiers (CNOAs, where the N denotes the number of operational amplifiers) in 1981. A composite op amp is a circuit with more than one op amp that permits the entire group of amplifiers to perform as a single amplifier with improved characteristics. [Ref 11:p.34]

Initial investigations into the CNOA behavior have been discussed in the literature [Refs. 6-11]. In general, the procedure used for developing CNOAs stemmed from creating possible circuit topologies that met the below-listed performance criteria:

1. Of the 136 possible circuit combinations using two operational amplifiers, or C2OAs, the denominator coefficients should satisfy the Routh-Horowitz criterion in that all coefficients be of the same sign. Additionally, in order to desensitize the C2OA with respect to its components, no numerator or denominator coefficient should be realized through differences.

2. The terminals of the C2OA should resemble as closely as possible those of the single op amp.
3. In order to achieve minimum phase shifts, no closed loop zeros should appear in the right-half of the s-plane.
4. The improved frequency, gain, and phase performance over the single operational amplifier should be enough to justify the increased number of op amps.

From the criteria listed above, the C2OA's insensitivity to active components, passive components, and op amps makes the C2OA attractive for use in circuits that must be designed to resist radiation degradation; the degradation of individual circuit/op amp parameters such as gain, slew rate and 3dB frequency will have less of an effect on circuits which utilize C2OAs than on those which use single op amps. Of the possible 136 C2OA circuit combinations, the four listed in Figure 5.3 [Ref 6:p. 451] proved superior.

Following the same approach, Composite Multiple Operational Amplifiers (CNOAs) were developed to further extend the operational frequencies at the expense of additional amplifiers. C3OAs were obtained by starting with one of the four proposed C2OAs while replacing one of its single op amps with any of the four C2OAs. C4OAs were developed similarly with each of the C2OA single op amps replaced with any of the four C2OAs, or by replacing a single op amp of the C3OAs by a C2OA. The reader interested in CNOAs with  $N > 2$  are referred to References 6 through 10, as only C2OAs were analyzed in this research. Figure 5.3 displays the circuits of C2OA-1 through C2OA-4. As only C2OA-1 was used for comparison in this thesis, further CNOA discussion will be focused accordingly.

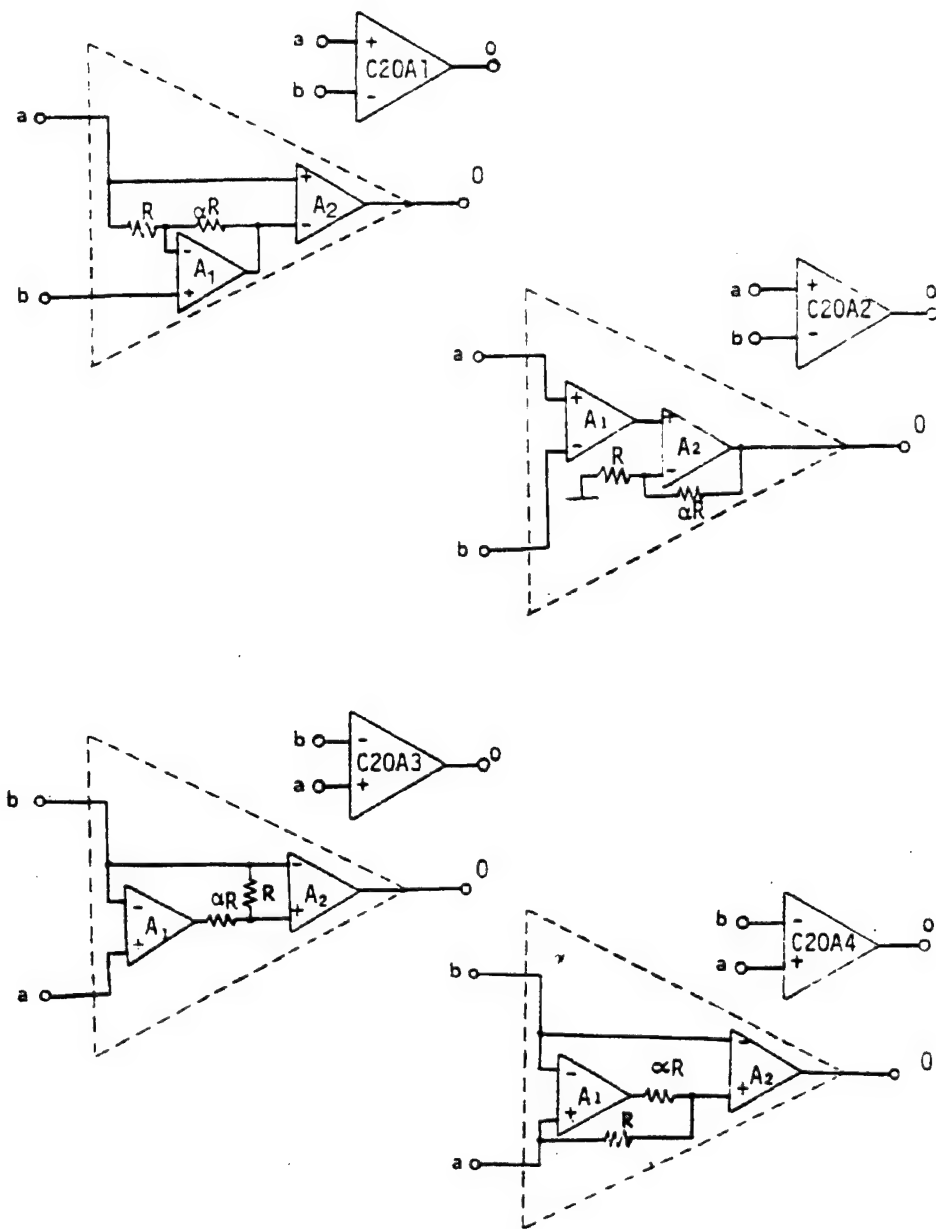


Figure 5.3 C2OAs

### C. COMPOSITE VERSUS SINGLE OP AMPS IN FINITE GAIN APPLICATIONS

Finite gain amplifiers are used in instrumentation, oscillators, and RC active filters. Ideally, the gain of these amplifiers should be constant with respect to frequency, however, due to the use of high gain op amps in their construction, they are bandwidth limited. These op amps have frequency dependent magnitude and phase characteristics which can cause the circuit response to change, or even become unstable. One way to overcome this problem is to improve circuit performance by the use of actively compensated op amps that have superior characteristics, such as CNOAs [Ref 9:pp. 31-32].

Using the same single-pole representation as in the single op amp gain equation, the open loop input-output relationship for C2OAs is

$$V_{oi} = V_a A_{ai}(s) - V_b A_{bi}(s)$$

where  $i$  denotes the type of C2OA, and  $A_a$  and  $A_b$  are the positive and negative open loop gains, respectively. It may be shown that, for the C2OA-1, equation 1 corresponds to

$$V_{o1} = V_a \frac{A_2(1+A_1)(1+\alpha)}{A_1(1+\alpha)} - V_b \frac{A_1 A_2(1+\alpha)}{A_1(1+\alpha)}$$

where  $\alpha$  is referred to as the *compositing resistor ratio* of C2OA-1, as shown above in Figure 5.3. If both single op amps are identical, i.e.,  $A_1=A_2=A_o$ , and the C2OA-1 is configured for a single-ended inverting application, then

$$A_{o(C2OA-1)} = -\frac{A_o^2(1+\alpha)}{A_o + (1+\alpha)} \cong A_o(1+\alpha) \quad \text{for } (1+\alpha) \ll A_o$$

which is the open-loop dc gain for a C2OA-1 inverting amplifier. The C2OA-1 will have a single pole roll-off from the pole at  $\omega_i/A_o$  to the pole at  $\omega_i/(1+\alpha)$ . Once again, it can be shown that the transfer function, assuming ideal op amps, for an inverting amplifier is

$$\frac{-k}{1+(s/\omega_p Q_p) + (s^2/\omega_p^2)}$$

$$\text{where} \quad \omega_p = \sqrt{\frac{\omega_1 \omega_2}{1+k}} \quad \text{and} \quad Q_p = \sqrt{\frac{\omega_1}{\omega_2(1+k)}} (1+\alpha)$$

Low sensitivity to circuit parameters is guaranteed since none of the numerator or denominator coefficients is realized through differences. Additionally, the coefficients in the denominator are always positive, guaranteeing stability. Hence, single op amps with mismatched gain bandwidth products ( $f_t$ s) within practical ranges can be used without appreciably affecting the stability or sensitivity of the finite gain realizations. Simultaneously designing for a maximally flat configuration and invoking the Routh-Horowitz stability criterion yields

$$Q_p = \frac{1}{\sqrt{2}} \quad \text{and} \quad \alpha + 1 > \frac{\sqrt{1+k}}{2}$$

where  $\alpha = \sqrt{\frac{1+k}{2}}$  is chosen, and  $k$  is the overall gain of the circuit utilizing the C2OA-1.

[Ref 6:pp. 449-455]

#### D. BANDWIDTH IMPROVEMENTS USING C2OA-1 IN FINITE GAIN APPLICATIONS AND THE IMPLICATIONS FOR RADIATION TOLERANCE

When using a single op amp for a finite gain amplifier, the bandwidth shrinks to approximately  $(w_i)/k$ . Using two single op amps cascaded together for finite gain amplification, the maximally flat 3dB bandwidth is obtained when each amplifier has a gain of

$$A = \sqrt{k}$$

in order to realize an overall gain of  $k$ . The resulting bandwidth shrinks to

$$A = .66w_i / \sqrt{k}$$

The C2OA-1s may be designed to shrink to only  $w_i / \sqrt{k}$  for the maximally flat value of  $Q = .707$ . Figure 5.4 [Ref 11:p. 48] reveals the improved bandwidth. [Ref. 6:p. 455]

The large increase in bandwidth provided by composite op amps could be important when the full frequency range of a single op amp is required during its operation in a damaging radiation environment. The composite op amp would have to undergo severe damage before its operating frequency range is reduced to that of a single op amp. Combining this advantage with the fact mentioned earlier that composite op amps are less sensitive to active circuit parameters, it is clear that composite op amps are good candidates for use in radiation environments.

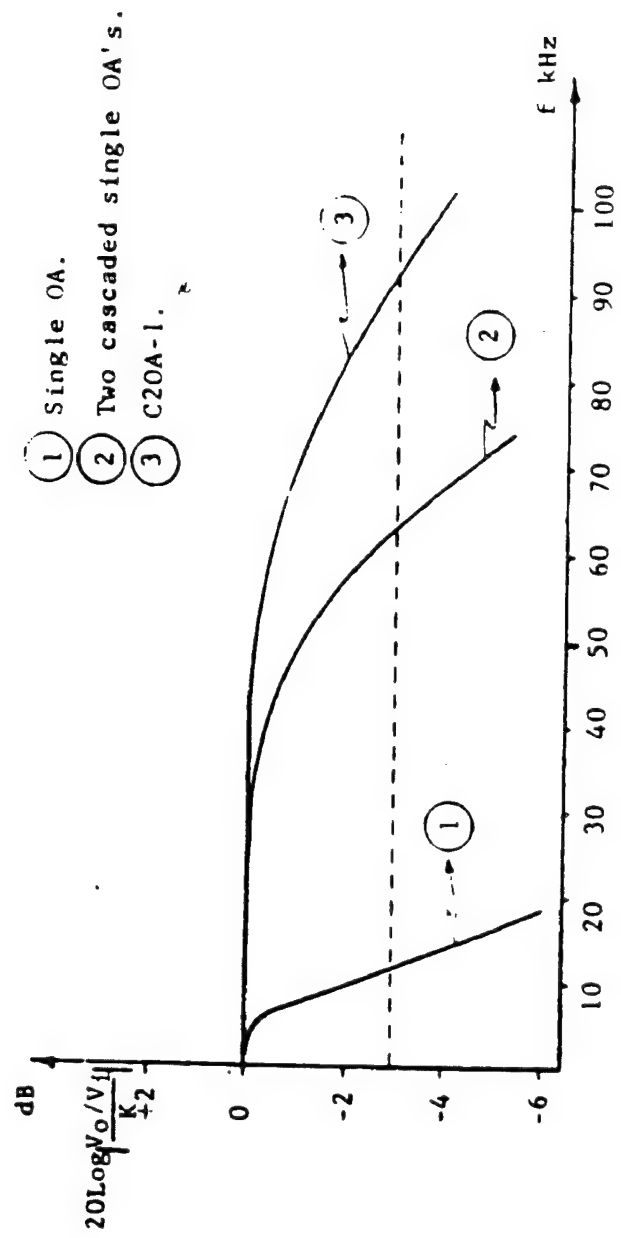


Figure 5.4 Bandwidth of C2OAs



## VI. RADIATION EFFECTS ON OPERATIONAL AMPLIFIERS

Op amps are relatively sensitive to total dose effects. Op amp gain, 3dB frequency, and slew rate are some of the parameters affected. [Ref. 19: pp. 41-32-41-35]

In previous research, BJT composite and single operational amplifiers were irradiated using a 30 MeV electron beam linear accelerator (LINAC), where in-situ gain, slew rate, and 3dB frequency were measured to ensure irradiated op amps were not given the opportunity to anneal. The op amps tested were Harris HS-5104RH (rad hard) and HA-5104. The non rad hard op amps are a general purpose op-amp with low noise and high performance (3 V/ $\mu$ s slew rate and 8 MHz gain bandwidth product), and they were all selected from the same lot. [Ref. 11:pp. 49-60]

While composite op amps have more ideal characteristics than single op amps in general, results from the previous LINAC testing (up to 68M rads(Si)) revealed that composite op amps also degraded at a slower pace (percentage-wise) than the single op amp response in both 3dB frequency and gain. This was true during the testing of both rad hard and non rad hard components. The difference in percentage was approximately 5% in gain and 15% in 3dB frequency for both types of components. Normalized gain and 3dB frequency for a total dose of 6M rads(Si) for non rad hard op amps, and 18M and 68M for rad hard op amps are displayed in Figures 6.1 through 6.3 [Ref. 11:pp. 72-73]. That the slew rate degradation of the composite op amps was less than that of the single op amps was surprising, as it was predicted that the degradation would be the same. [Ref. 11:pp. 70-74]

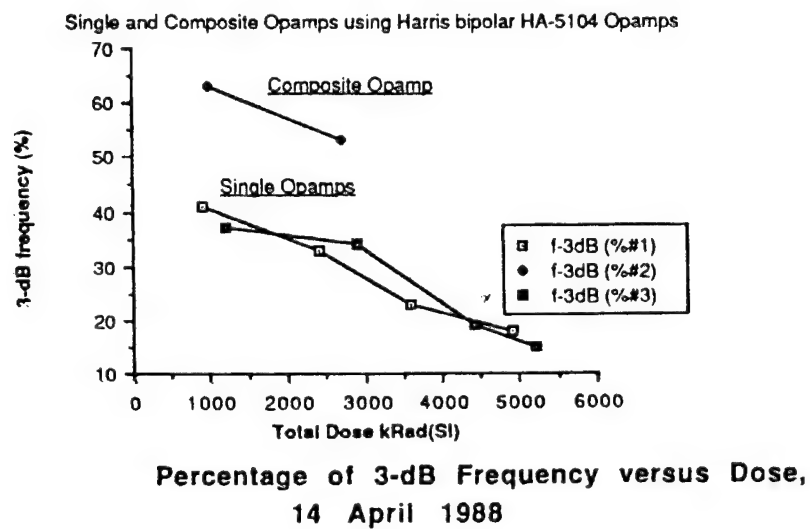
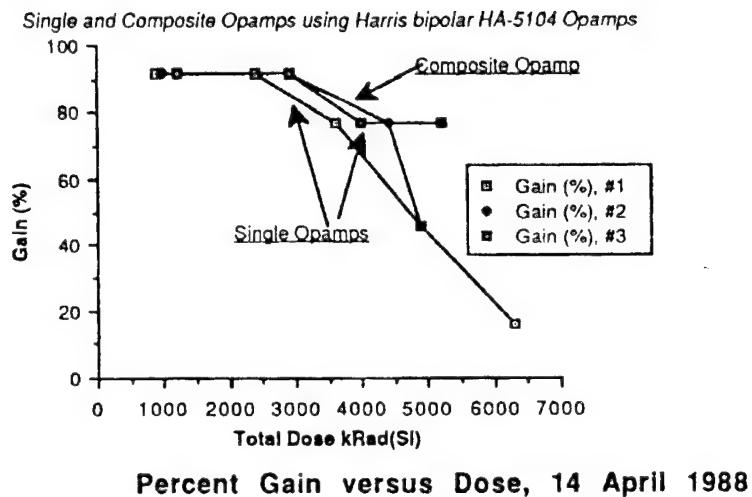


Figure 6.1 Non Rad Hard Op Amp Response to 6M rads(Si) Using a LINAC

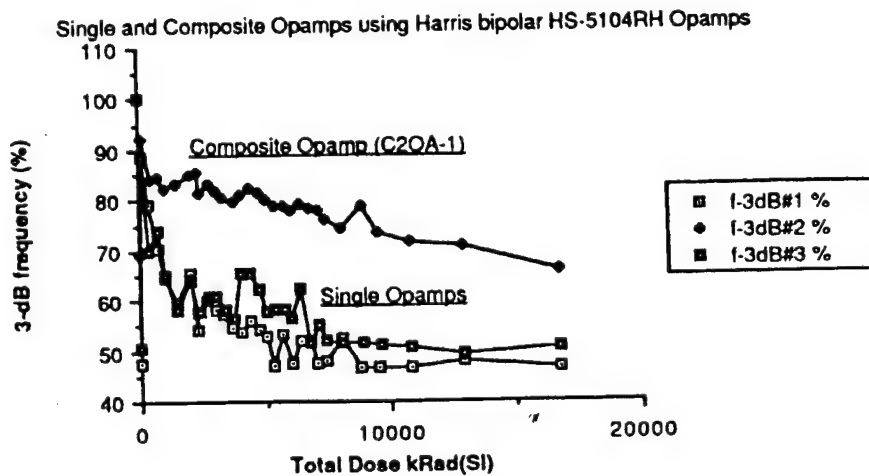
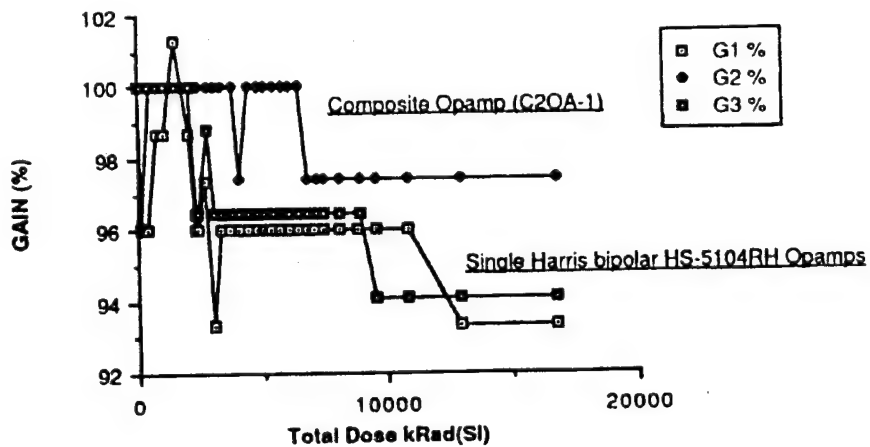


Figure 6.2 Rad Hard Op Amp Response to 18M rads(Si) Using a LINAC

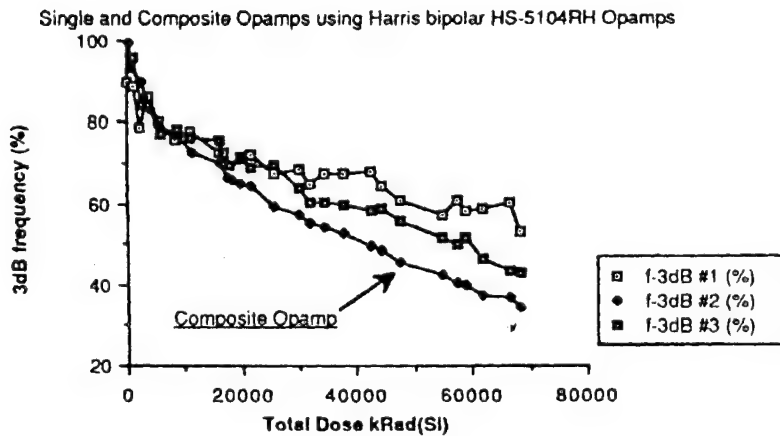
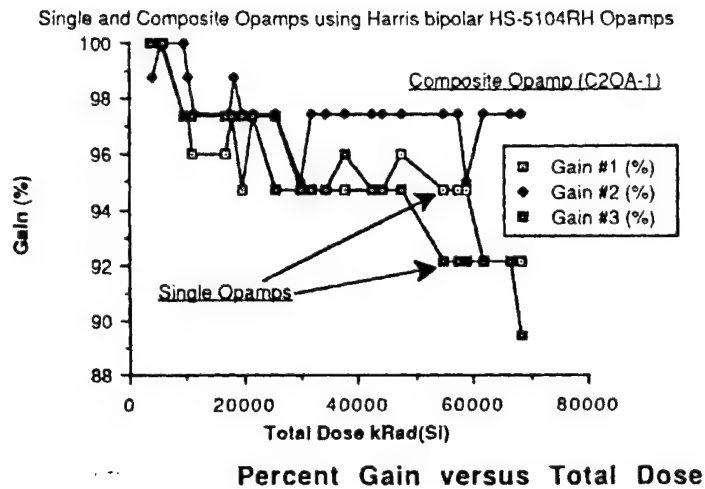


Figure 6.3 Rad Hard Op Amp Response to 68M rads(Si) using a LINAC

During the LINAC irradiation test of single and composite op amps in the previous research, it was surprising to discover that the slew rate of the composite op amp was faster than of the single amplifier under the same conditions. It was also surprising to discover that the rad hard devices, composite and single, survived a total dose of over 68M rads(Si) with a drop of only 5-10% in gain and a 50-60% drop in 3dB frequency (or bandwidth). The op amp performance is guaranteed by the manufacturer at 100k rads.

Incidentally, Figure 6.1 is a prime example of how unique device response to radiation can be: even the LINAC-irradiated twin op amps on the same chip did not degrade similarly.

## **VII. SIMULATION PROCEDURE**

To simulate the effect of radiation degradation on op amp parameters, the following technique is introduced. The main concept in this technique is to generate correspondences between 1) transistor parameter variations and total dose radiation, and 2) transistor parameter variations and circuit response, so that a combination of the two, in turn, would correlate the relationship between circuit response and total dose radiation. The correspondence between transistor parameter variations and total dose radiation was already described in Chapter IV, specifically in Figures 4.2 and 4.4. A correspondence between transistor parameter variations and circuit response was obtained through iterating the same inverting amplifier configuration response several times using different transistor parameter values, for which the procedure is discussed in this chapter.

### **A. OP AMP MODELS**

The first step was to choose both BJT and CMOS op amp models for use in both the single and composite op amp configurations. Two models were selected from Sedra and Smith [Ref. 5] due to their simplicity, popularity, and availability of their devices' PSPICE parameters. The BJT and CMOS op amp circuit layouts used in this simulation are displayed respectively in Figure 7.1, which was adapted from Figure 5.1, and Figure 7.2 [Ref. 5:p. C-6], followed by their associated PSPICE programs.

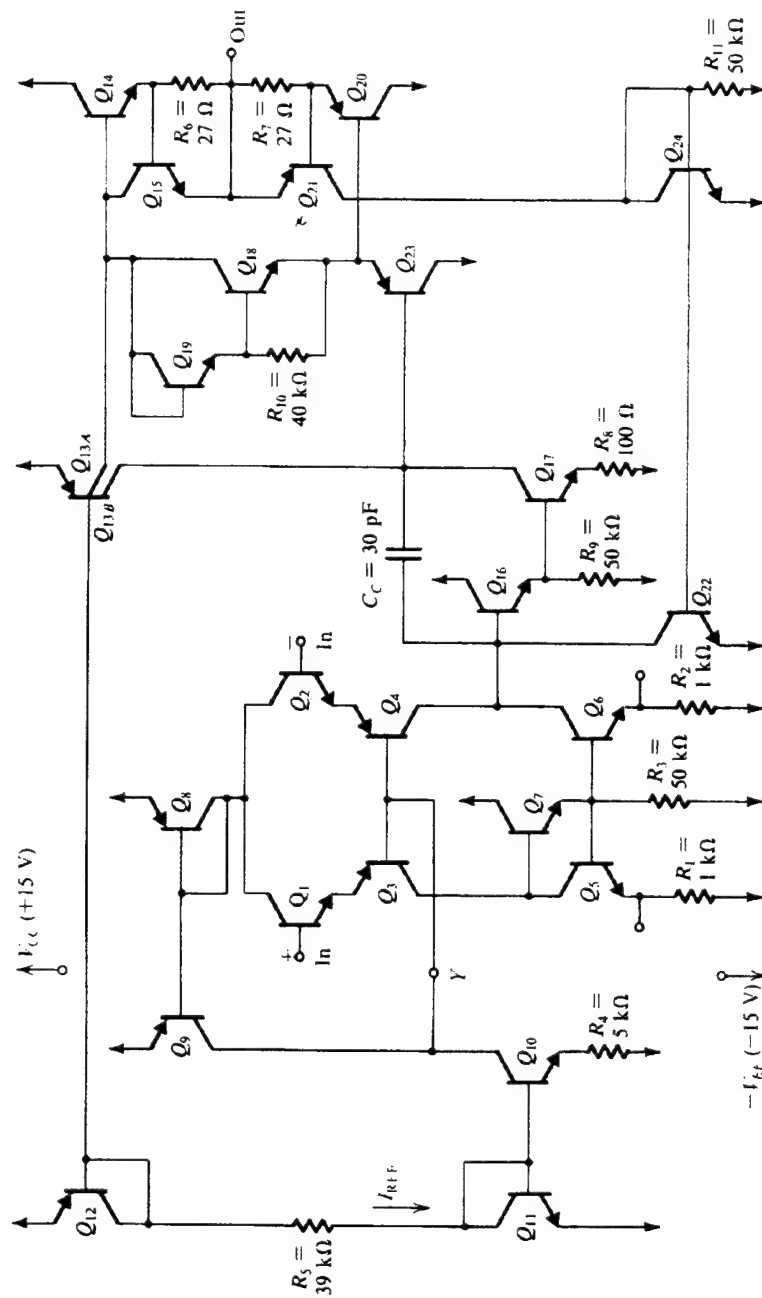


Figure 7.1 BJT Op Amp Circuit

# \*741 OP AMP PSPICE CIRCUIT

```
.SUBCKT OPAMP 5,14,19
VCC 1 0 15
VEE 26 0 -15
Q1 12 5 8 MOD2
Q2 12 14 7 MOD2
Q3 10 6 8 MOD1
Q4 15 6 7 MOD1
Q5 10 13 11 MOD2
Q6 15 13 16 MOD2
Q7 1 10 13 MOD2
Q8 12 12 1 MOD1
Q9 6 12 1 MOD1
Q10 6 3 4 MOD2
Q11 3 3 26 MOD2
Q12 2 2 1 MOD1
Q13 17 2 1 MOD3
Q14 1 17 22 MOD5 3
Q15 17 22 19 MOD2
Q16 1 15 9 MOD2
Q17 18 9 25 MOD2
Q18 17 20 21 MOD2
Q19 17 17 20 MOD2
Q20 26 21 23 MOD6 3
Q21 24 23 19 MOD1
Q22 15 24 26 MOD2
Q23 26 18 21 MOD1
Q24 24 24 26 MOD2
Q25 18 2 1 MOD4
R1 11 26 1K
R2 16 26 1K
R3 13 26 50K
R4 4 26 5K
R5 2 3 39K
R6 22 19 27
R7 19 23 27
R8 25 26 100
R9 9 26 50K
R10 20 21 40K
R11 24 26 50K
C1 15 18 30P
.MODEL MOD1 PNP(BF=50 IS=10F CJE=.1F CJC=1.05P CJS=5.1P)
.MODEL MOD2 NPN(BF=200 IS=10F CJE=.65F CJC=.36P CJS=3.2P)
.MODEL MOD3 PNP(BF=50 IS=2.5F CJE=.1F CJC=.3P CJS=4.8P)
.MODEL MOD4 PNP(BF=50 IS=7.5F CJE=.1F CJC=.9P CJS=4.8P)
.MODEL MOD5 NPN(BF=200 IS=10F CJE=2.8F CJC=1.55P CJS=7.8P)
.MODEL MOD6 PNP(BF=50 IS=10F CJE=4.05F CJC=2.8P)
.ENDS OPAMP
```





```
.ENDS CMOSOPAMP
```

## **B. OP AMPS IN THE INVERTING AMPLIFIER CONFIGURATION**

The inverting amplifier configuration was chosen because it is simple and provided a comparison with previous research (Sage). Since radiation degradation in transistors is dependent on bias, it was important to have roughly the same input voltage as Sage's circuit to produce a useful comparison. Sage's input voltage was 4mV V<sub>p</sub> with an overall gain of 200. A circuit with an input voltage of 10mV V<sub>p</sub> AC and inverting amplifier gain of 100 for an output gain of 1V was chosen in this thesis.

## **C. RADIATION SIMULATION**

### **1. Gain and 3dB Degradation**

In simulating ionizing radiation in both BJT and CMOS transistors, the current gain (PSPICE code BF) and threshold voltages (PSPICE code VTO) were changed, respectively, within each transistor of each circuit.  $\beta$  was varied from 0% to 97.5% degradation in both NPN and PNP transistors, corresponding to respective drops from 200 to 6, and 100 to 3. Each BJT op amp circuit simulation was executed seven times with decreases in  $\beta$  of 0%, 50%, 90%, 95%, 96%, 97%, and 97.5%. In order to preserve data points for the nonlinear portion of the degradation curves, a large discontinuity between  $\beta$  degradation of 0% and 90% was allowed since little change in op amp response was noted between these data points. The value of 97.5% was selected as the end point since  $\beta$  degradation beyond this point destabilized the circuit, for both single and composite op amps.

In the CMOS op amps,  $V_t$  was altered from 1V to -1V, and from -1V to -3V for NMOS and PMOS transistors, respectively. Since the CMOS components are more sensitive to ionizing radiation, with smaller changes in parameters, more regularly spaced  $V_t$  degradation data points were selected than for the BJT transistors. Degradation points of  $V_t$ ,  $V_t-0.25V$ ,  $V_t-0.5V$ ,  $V_t-1V$ ,  $V_t-1.25V$ ,  $V_t-1.5V$ , and  $V_t-2V$  were selected, after which the circuit for both single and composite op amps became unstable.

An AC analysis was conducted in PSPICE for each inverting amplifier circuit which corresponded to a particular degradation value of  $\beta$  and of  $V_t$ . The programs for single and composite BJT and CMOS op amps are given below. After running each circuit for each data point, the voltage output was extracted into two sets of data, with frequency as the first column, and output voltage (in dB) at node 3 in the second column. Keeping in mind that CMOS data processing paralleled that of the BJT data, programs for loading and processing only BJT data are provided below. Data for all circuits was gathered in a MATLAB file similar to the program entitled *MATLAB LOADING PROGRAM* and arranged in a matrix where rows one through fourteen contained single op amp circuit data (frequency and voltage) for each of seven  $\beta$  degradation points, and rows fifteen through twenty-eight contained associated composite op amp data.

This large data matrix was transferred to a second MATLAB file, such as the program entitled *MATLAB GAIN AND 3dB PROCESSING PROGRAM* below, which processed the matrix to obtain gain and 3dB frequencies, and then saved the result. To obtain the inverting amplifier finite gain for each frequency interval in dB, the input voltage of 10mV was converted to dB, then subtracted from the output voltage. The 3dB

\*PSPICE BJT SINGLE OP AMP (741) INVERTING  
 \*CONFIGURATION SHOWING BETA CHANGES

.SUBCKT OPAMP

```

.
.
.
*0% DEGRADATION
.MODEL MOD1 PNP(BF=50 IS=10F CJE=.1F CJC=1.05P CJS=5.1P)
.MODEL MOD2 NPN(BF=200 IS=10F CJE=.65F CJC=.36P CJS=3.2P)
.MODEL MOD3 PNP(BF=50 IS=2.5F CJE=.1F CJC=.3P CJS=4.8P)
.MODEL MOD4 PNP(BF=50 IS=7.5F CJE=.1F CJC=.9P CJS=4.8P)
.MODEL MOD5 NPN(BF=200 IS=10F CJE=2.8F CJC=1.55P CJS=7.8P)
.MODEL MOD6 PNP(BF=50 IS=10F CJE=4.05F CJC=2.8P)
%50% DEGRADATION
.MODEL MOD1 PNP(BF=25 IS=10F CJE=.1F CJC=1.05P CJS=5.1P)
.MODEL MOD2 NPN(BF=100 IS=10F CJE=.65F CJC=.36P CJS=3.2P)
.MODEL MOD3 PNP(BF=25 IS=2.5F CJE=.1F CJC=.3P CJS=4.8P)
.MODEL MOD4 PNP(BF=25 IS=7.5F CJE=.1F CJC=.9P CJS=4.8P)
.MODEL MOD5 NPN(BF=100 IS=10F CJE=2.8F CJC=1.55P CJS=7.8P)
.MODEL MOD6 PNP(BF=25 IS=10F CJE=4.05F CJC=2.8P)
*90% DEGRADATION
.MODEL MOD1 PNP(BF=5 IS=10F CJE=.1F CJC=1.05P CJS=5.1P)
.MODEL MOD2 NPN(BF=20 IS=10F CJE=.65F CJC=.36P CJS=3.2P)
.MODEL MOD3 PNP(BF=5 IS=2.5F CJE=.1F CJC=.3P CJS=4.8P)
.MODEL MOD4 PNP(BF=5 IS=7.5F CJE=.1F CJC=.9P CJS=4.8P)
.MODEL MOD5 NPN(BF=20 IS=10F CJE=2.8F CJC=1.55P CJS=7.8P)
.MODEL MOD6 PNP(BF=5 IS=10F CJE=4.05F CJC=2.8P)
*95% DEGRADATION
.MODEL MOD1 PNP(BF=2.5 IS=10F CJE=.1F CJC=1.05P CJS=5.1P)
.MODEL MOD2 NPN(BF=10 IS=10F CJE=.65F CJC=.36P CJS=3.2P)
.MODEL MOD3 PNP(BF=2.5 IS=2.5F CJE=.1F CJC=.3P CJS=4.8P)
.MODEL MOD4 PNP(BF=2.5 IS=7.5F CJE=.1F CJC=.9P CJS=4.8P)
.MODEL MOD5 NPN(BF=10 IS=10F CJE=2.8F CJC=1.55P CJS=7.8P)
.MODEL MOD6 PNP(BF=2.5 IS=10F CJE=4.05F CJC=2.8P)
*96% DEGRADATION
.MODEL MOD1 PNP(BF=2 IS=10F CJE=.1F CJC=1.05P CJS=5.1P)
.MODEL MOD2 NPN(BF=8 IS=10F CJE=.65F CJC=.36P CJS=3.2P)
.MODEL MOD3 PNP(BF=2 IS=2.5F CJE=.1F CJC=.3P CJS=4.8P)
.MODEL MOD4 PNP(BF=2 IS=7.5F CJE=.1F CJC=.9P CJS=4.8P)
.MODEL MOD5 NPN(BF=8 IS=10F CJE=2.8F CJC=1.55P CJS=7.8P)
.MODEL MOD6 PNP(BF=2 IS=10F CJE=4.05F CJC=2.8P)
*97% DEGRADATION
.MODEL MOD1 PNP(BF=1.5 IS=10F CJE=.1F CJC=1.05P CJS=5.1P)
.MODEL MOD2 NPN(BF=6 IS=10F CJE=.65F CJC=.36P CJS=3.2P)
.MODEL MOD3 PNP(BF=1.5 IS=2.5F CJE=.1F CJC=.3P CJS=4.8P)
.MODEL MOD4 PNP(BF=1.5 IS=7.5F CJE=.1F CJC=.9P CJS=4.8P)
.MODEL MOD5 NPN(BF=6 IS=10F CJE=2.8F CJC=1.55P CJS=7.8P)
.MODEL MOD6 PNP(BF=1.5 IS=10F CJE=4.05F CJC=2.8P)
.ENDS OPAMP

```

\*PSPICE BJT SINGLE OP AMP (741) INVERTING  
 \*CONFIGURATION SHOWING BETA CHANGES CONTD.

\*INVERTING AMPLIFIER CIRCUIT

```

X1  0 2 3  OPAMP
VIN 4 0 AC .01                      *gain analysis AC input
VIN 4 0 PULSE(0 .01 10U 1N 1N .13M .26M) *slew rate input
Rin 2 4 1e3
Rout 2 3 1e5

```

\*PLOT ANALYSIS

```

.AC DEC 40 1e3HZ 1e6HZ              *gain AC analysis
.PRINT AC VDB(3,0)
.PLOT AC VDB(3,0)
.TRAN 5U .3M                        *slew rate analysis
.PRINT TRAN V(3) V(4)
.PLOT TRAN V(3) (0,-1) V(4) (0,.01)

```

.END

\*COMPOSITE (C2OA1) BIPOLAR OP AMP INVERTING CONFIGURATION

```

.SUBCKT OPAMP                      *refer to single bjt op amp program

```

```

.ENDS OPAMP

```

\*C2OA1 CIRCUIT

```

.SUBCKT C2OA1 1,2,3
X1 2 4 5 OPAMP
X2 1 5 3 OPAMP
R1 4 1 1K
R2 5 4 6.1K
.ENDS C2OA1

```

\*INVERTING AMPLIFIER CIRCUIT

```

X1  0 2 3  C2OA1
VIN 4 0 AC .01                      *gain AC input
VIN 4 0 PULSE(0 .01 10U 1N 1N .13M .26M) *slew rate input
Rin 2 4 1e3
Rout 2 3 1e5

```

\*PLOT ANALYSIS

```

.AC DEC 40 1e3HZ 1e6HZ              *gain AC analysis
.PRINT AC VDB(3,0)                  *
.PLOT AC VDB(3,0)                  *
.TRAN 5U .3M                        *slew rate analysis
.PRINT TRAN V(3) V(4)              *
.PLOT TRAN V(3) (0,-1) V(4) (0,.01) *

```

.END

frequency was determined by finding the frequency, indexed by n3db in the code, whose data point came closest to the value of (0dB frequency minus 3dB). Then percentages of gain and of 3dB were calculated for comparison with previous results. Since the op amps simulated were different from those actually irradiated, a relative or percentage comparison was more appropriate and yielded better results than a straight comparison.

## **2. Slew Rate Degradation**

As mentioned previously, in order to obtain slew rate data, separate source and analysis lines were needed which were commented with \* in the programs presented below. Again, an AC analysis was conducted, where the output constitutes three columns of data: time, Vout, and Vin.

After loading data using the same procedure discussed above, the data was then arranged in a matrix where rows one through twenty-one contained single op amp circuit data (time, Vout, and Vin) for each of seven  $\beta$  degradation points, and rows twenty-two through forty-two contained associated composite op amp data. This huge matrix was then transferred into a second file for processing, where the maximum slew rate was obtained by taking the maximum of the voltage difference divided by the time difference for each time interval.

\*PSPICE CMOS SINGLE OPAMP INVERTING AMPLIFIER  
\*CONFIGURATION

.SUBCKT CMOSOPAMP 2,1,7

VDD 10 0 DC 5  
VSS 9 0 DC -5  
IREF 6 9 DC 25U  
M1 4 1 3 10 2 L=8U W=120U  
M2 5 2 3 10 2 L=8U W=120U  
M3 4 4 9 9 1 L=10U W=50U  
M4 5 4 9 9 1 L=10U W=50U  
M5 3 6 10 10 2 L=10U W=150U  
M6 7 5 9 9 1 L=10U W=100U  
M7 7 6 10 10 2 L=10U W=150U  
M8 6 6 10 10 2 L=10U W=150U  
CC 5 8 10PF  
RC 8 7 10K  
CL 7 0 10PF

\*NO DEGRADATION

.MODEL 1 NMOS (LEVEL=2 VTO=1 KP=20U LAMBDA=0.04)  
.MODEL 2 PMOS (LEVEL=2 VTO=-1 KP=10U LAMBDA=0.04)

\*-.25V DEGRADATION

.MODEL 1 NMOS (LEVEL=2 VTO=.75 KP=20U LAMBDA=0.04)  
.MODEL 2 PMOS (LEVEL=2 VTO=-1.25 KP=10U LAMBDA=0.04)

\*-.5V DEGRADATION

.MODEL 1 NMOS (LEVEL=2 VTO=.5 KP=20U LAMBDA=0.04)  
.MODEL 2 PMOS (LEVEL=2 VTO=-1.5 KP=10U LAMBDA=0.04)

\*-2V DEGRADATION

.MODEL 1 NMOS (LEVEL=2 VTO=-1 KP=20U LAMBDA=0.04)  
.MODEL 2 PMOS (LEVEL=2 VTO=-3 KP=10U LAMBDA=0.04)

.ENDS CMOSOPAMP

\*INVERTING AMPLIFIER CIRCUIT

X1 0 2 3 CMOSOPAMP  
VIN 4 0 AC .01 \*gain AC input  
VIN 4 0 PULSE(0 .01 10U 1N 1N .13M .26M) \*slew rate input  
Rin 2 4 1e3  
Rout 2 3 1e5

\*PLOT ANALYSIS

.AC DEC 40 1e3HZ 1e6HZ \*gain AC analysis  
.PRINT AC VDB(3,0)  
.PLOT AC VDB(3,0)  
.TRAN 5U .3M \*slew rate analysis  
.PRINT TRAN V(3) V(4)  
.PLOT TRAN V(3) (0,-1) V(4) (0,.01)

\*PSPICE CMOS COMPOSITE (C2OA1) OPAMP INVERTING  
 \*AMPLIFIER CONFIGURATION

.SUBCKT CMOSOPAMP 2,1,7 *\*refer to single cmos op amp program*

.ENDS CMOSOPAMP

\*C2OA1 CIRCUIT

.SUBCKT C2OA1 1,2,3  
 X1 2 4 5 CMOSOPAMP  
 X2 1 5 3 CMOSOPAMP  
 R1 4 1 1K  
 R2 5 4 6.1K  
 .ENDS C2OA1

\*INVERTING AMPLIFIER CIRCUIT

X1 0 2 3 C2OA1  
 VIN 4 0 AC .01 *\*gain AC input*  
 VIN 4 0 PULSE(0 .01 10U 1N 1N .13M .26M) *\*slew rate input*  
 Rin 2 4 1e3  
 Rout 2 3 1e5

\*PLOT ANALYSIS

.AC DEC 40 1e3HZ 1e6HZ *\*gain AC analysis*  
 .PRINT AC VDB(3,0) *\**  
 .PLOT AC VDB(3,0) *\**  
 .TRAN 5U .3M *\*slew rate analysis*  
 .PRINT TRAN V(3) V(4) *\**  
 .PLOT TRAN V(3) (0,-1) V(4) (0,.01) *\**

.END



# %MATLAB LOADING PROGRAM

%THIS PROGRAM LOADS DATA OF BIPOLAR (BI) JUNCTION  
%TRANSISTORS AND CMOS (CM) IN ORDER TO PROCESS GAIN DATA

```
load b:\thesis\gain\oa bi(:,1:2)=oa;
load b:\thesis\gain\oad50 bi(:,3:4)=oad50;
load b:\thesis\gain\oad90 bi(:,5:6)=oad90;
load b:\thesis\gain\oad95 bi(:,7:8)=oad95;
load b:\thesis\gain\oad96 bi(:,9:10)=oad96;
load b:\thesis\gain\oad97 bi(:,11:12)=oad97;
load b:\thesis\gain\oad975 bi(:,13:14)=oad975;
load b:\thesis\gain\c2oa1 bi(:,15:16)=c2oa1;
load b:\thesis\gain\c2oa1d50 bi(:,17:18)=c2oa1d50;
load b:\thesis\gain\c2oa1d90 bi(:,19:20)=c2oa1d90;
load b:\thesis\gain\c2oa1d95 bi(:,21:22)=c2oa1d95;
load b:\thesis\gain\c2oa1d96 bi(:,23:24)=c2oa1d96;
load b:\thesis\gain\c2oa1d97 bi(:,25:26)=c2oa1d97;
load b:\thesis\gain\c2oa1d99 bi(:,27:28)=c2oa1d99;

save bi.m bi -ascii

load b:\thesis\gain\cmos; cm(:,1:2)=cmos;
load b:\thesis\gain\cmosd25; cm(:,3:4)=cmosd25;
load b:\thesis\gain\cmosd50; cm(:,5:6)=cmosd50;
load b:\thesis\gain\cmosd100; cm(:,7:8)=cmosd100;
load b:\thesis\gain\cmosd125; cm(:,9:10)=cmosd125;
load b:\thesis\gain\cmosd150; cm(:,11:12)=cmosd150;
load b:\thesis\gain\cmosd200; cm(:,13:14)=cmosd200;
load b:\thesis\gain\cmosd300; cm(:,15:16)=cmosd300;
load b:\thesis\gain\cc; cm(:,17:18)=cc;
load b:\thesis\gain\ccd25; cm(:,19:20)=ccd25;
load b:\thesis\gain\ccd50; cm(:,21:22)=ccd50;
load b:\thesis\gain\ccd100; cm(:,23:24)=ccd100;
load b:\thesis\gain\ccd125; cm(:,25:26)=ccd125;
load b:\thesis\gain\ccd150; cm(:,27:28)=ccd150;
load b:\thesis\gain\ccd200; cm(:,29:30)=ccd200;
load b:\thesis\gain\ccd300; cm(:,31:32)=ccd300;

save cm.m cm -ascii
```

# %MATLAB GAIN AND 3dB PROCESSING PROGRAM

%THIS PROGRAM FINDS GAINS AND 3dB FREQUENCIES FOR ALL CIRCUITS  
%WITHIN THE DATA MATRIX BI.M. THE CIRCUIT WITHIN WHICH ALL OP AMPS  
%WERE SIMULATED IS AN INVERTING AMPLIFIER WITH GAIN=100 USING A  
%RESISTOR RATIO OF 100K/1K AND Vin=10mV.

%bi.m is a matrix of n-by-m elements where odd m's contain  
%frequency data for each circuit and even m's contain Vout in  
%volts.

load bi.m; clear temp;

%DECLARE CONSTANTS

%Vin in dB (Vin=1mV)  
Vindb=20\*log10(.01);

%initiate matrix indices (n x m)  
m=1;n=2;n3db=2;k=1;

%zero-pad matrices

gaindb=zeros(n,size(bi,2)/2);  
pf3db=zeros(1,size(bi,2)/2);  
pgain=zeros(1,size(bi,2)/2);  
f3db=zeros(1,size(bi,2)/2);  
gain=zeros(1,size(bi,2)/2);  
gain3db=zeros(1,size(bi,2)/2);  
bidata=zeros(size(bi,2)/2,6);

%BEGIN ITERATIONS

%M ITERATES ACROSS ALL CIRCUITS  
for m=1:2:27

temp(:,1:2)=bi(:,m:m+1);

%CALCULATE GAIN, 3dB VOLTAGE AND 3dB FREQUENCY

%CALCULATE 0-HERTZ GAIN AS GAIN=Vout-Vin

gaindb(1,k)=temp(1,2)-Vindb;

%GAIN3db FINDS THE VOLTAGE AT WHICH THE 3dB FREQUENCY OCCURS

gain3db(k)=gaindb(1,k)-3.0000;

%N ITERATES DOWN THE DATA WITHIN EACH CIRCUIT

n3db=2;

for n=2:(length(temp)-1)

%CALCULATE GAIN FOR EACH FREQUENCY INTERVAL

gaindb(n,k)=temp(n,2)-Vindb;

%IF-END LOOP FINDS FREQUENCY WHICH IS CLOSEST

%MATCH TO 3dB

if (gain3db(k)-gaindb(n,k))<abs(gain3db(k)-gaindb(n3db,k))  
n3db=n;

%MATLAB GAIN AND 3dB PROCESSING PROGRAM (contd.)

%CALCULATE GAIN BANDWIDTH PRODUCT

%CONVERT FROM dB TO VOLTAGE

gain(k)=10^(gaindb(1,k)/20);

%RETRIEVE 3dB FREQUENCY

f3db(k)=temp(n3db,1);

%CALCULATE GAIN BANDWIDTH PRODUCT

gbwp(k)=f3db(k)\*gain(k);

%CALCULATE PERCENTAGES

%CALCULATE PERCENTAGES FOR SINGLE OAs

if k<8

pf3db(k)=(f3db(k)/f3db(1))\*100;

pgain(k)=(gain(k)/gain(1))\*100;

%CALCULATE PERCENTAGES FOR COMPOSITE OAs

else

pf3db(k)=(f3db(k)/f3db(8))\*100;

pgain(k)=(gain(k)/gain(8))\*100;

end

%STORE DATA

bidata(k,:)=[gain(k)pgain(k)gain3db(k)f3db(k)pf3db(k)gbwp(k)];

k=k+1;

end

save b:bidata bidata

save b:bigaindb gaindb

```

%MATLAB SLEWRATE PROCESSING PROGRAM

%THIS PROGRAM GENERATES INSTANTANEOUS AND MAXIMUM SLEWRATES

load b:\thesis\slewrates\bis.m;
clear z;

%DECLARE CONSTANTS
%count
m=1;n=2;k=0;

%BEGIN INTERATION
for m=1:3:40
    z(:,1:3)=bis(:,m:m+2);
    k=k+1;

    for n=2:(length(z))
        %DETERMINE INSTANTANEOUS SLEWRATES
        slewrates(k,n)=(z(n,2)-z((n-1),2))/(z(n,1)-z((n-1),1));
        %REMOVES INFINITE VALUES
        if slewrates(k,n)<1e10
            posr(k,n)=slewrates(k,n);
        else posr(k,n)=0;
        end
    end

    %DETERMINE MAXIMUM SLEWRATES
    maxsr(k)=max(abs(posr(k,:))); end
end

save slewrates slewrates -ascii
save maxsr maxsr -ascii

```

## VIII. RESULTS

When examining the results presented below, it is important to keep in mind that this is a crude simulation in that it considers only the radiation effects on major transistor parameters; there are a multitude of radiation effects which were not considered either because they were not quantifiable, or they were difficult to analyze, or both.

The main objective for both BJT and CMOS circuit simulations was to show that composite op amps offered a larger bandwidth than their single counterparts when irradiated. For the BJT circuits, results from a previous thesis [Ref. 11] which irradiated BJT components under a linear accelerator (LINAC) offered a comparison. Hence, a further objective was to validate the previous LINAC results by comparison with the normalized degradation response.

Insofar as CMOS components were concerned, no previous work on CMOS irradiation was available for comparison, so the results of the CMOS simulation are presented and offered for future comparison with experimental CMOS component irradiation.

### A. COMPOSITE VERSUS SINGLE OP AMPS

#### 1. Gain and 3dB Frequency

Figure 8.1, which provides gain degradation curves for both single and composite BJT op amps, shows the more ideal response the composite op amp offers over the single op amp. In fact, the composite op amp bandwidth is larger than that of

the single op amp by a factor of ten for this application. In Figures 8.2 through 8.5, the bandwidth characteristics are broken down in terms of 3dB frequency and gain bandwidth product ( $f_t$  or GBWP). In these figures, each op amp response lies between two curves. The curves are an outgrowth of  $\beta$ -to-total-dose mapping using Figure 4.2.

The CMOS circuit simulation results provided in Figures 8.6 through 8.10 mirrored those of the BJT circuit results discussed above, in that the composite op amps provided a much larger bandwidth; however, the bandwidth improvement over the single op amps was slightly smaller at a factor of eight, vice the ten discussed above.

A general comparison of all figures depicts the greater sensitivity CMOS components have to ionizing radiation compared to BJT components: the CMOS circuits withstood a total dose of only 50k rads(Si) whereas the BJT circuits were able to withstand at least 1M rads(Si) and up to 100M rads(Si).

## **2. Slew rates**

Figures 8.11 through 8.16 provide slewrate results in response to a pulse input for all circuits. In general, both the BJT and CMOS composite op amps provided a five-times-faster slewrate than their single op amp counterparts, validating the first observation of this phenomenon by Sage, who conducted the previous results. This is contrary to theory, which predicts the same slew rates under all conditions for both composite and single op amps. While there is no explanation for this yet, the faster slewrate has great implications for using composite op amps in high-speed, particularly digital, applications.

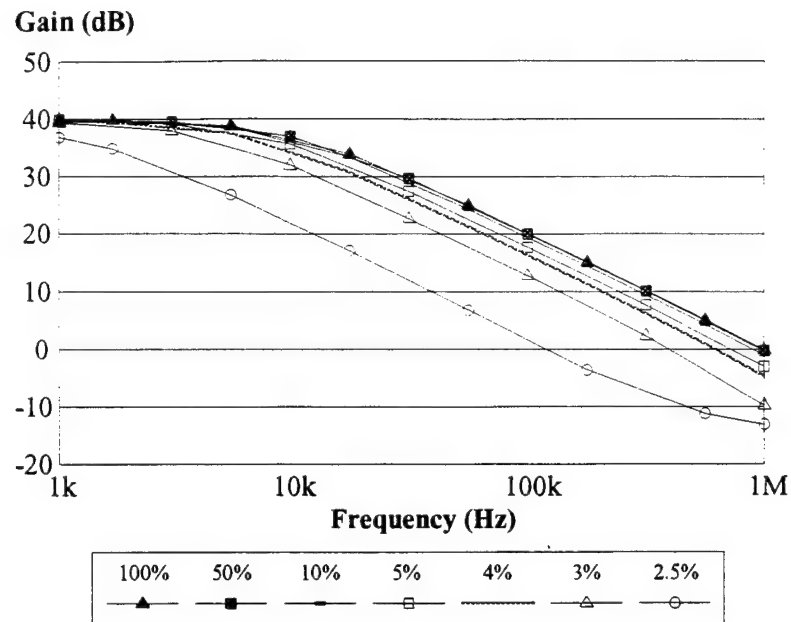


Figure 8.1a BJT Single Op Amp Degradation Curves versus Frequency as a Function of Percent Remaining Beta

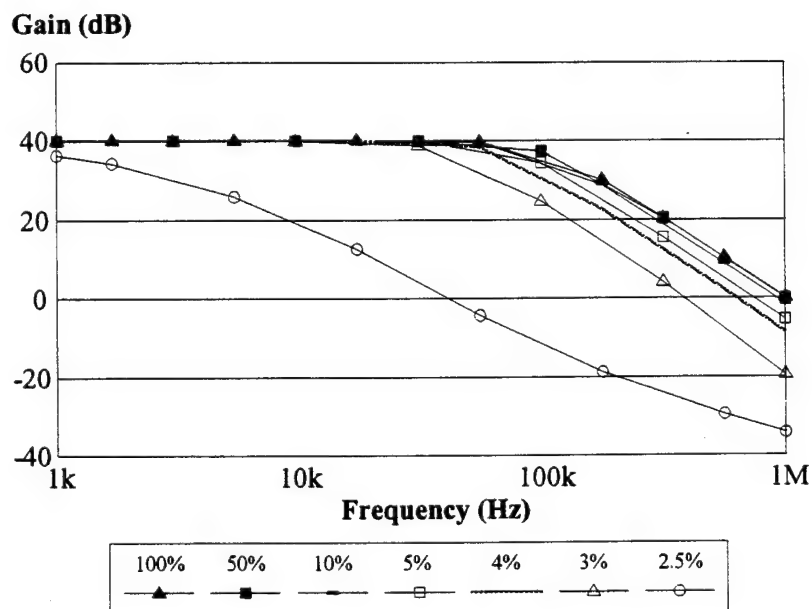


Figure 8.1b BJT Composite Op Amp Degradation Curves versus Frequency as a Function of Percent Remaining Beta

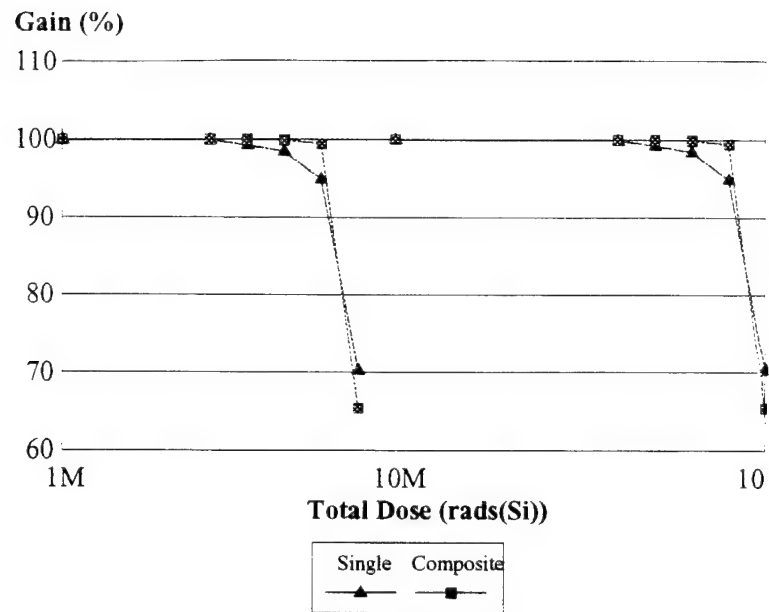


Figure 8.2 BJT Composite and Single Op Amp Gain versus Total Dose

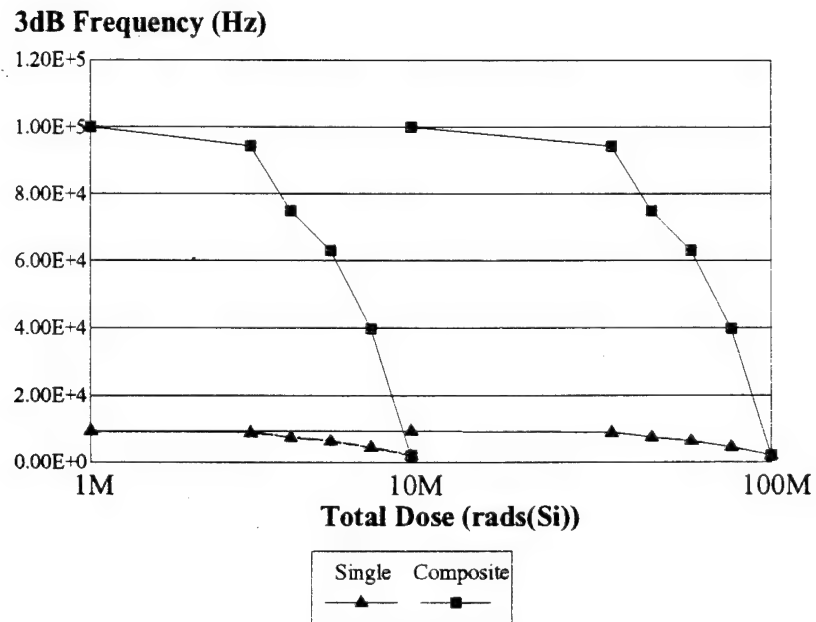


Figure 8.3 BJT Composite and Single Op Amp 3dB Frequency versus Total Dose



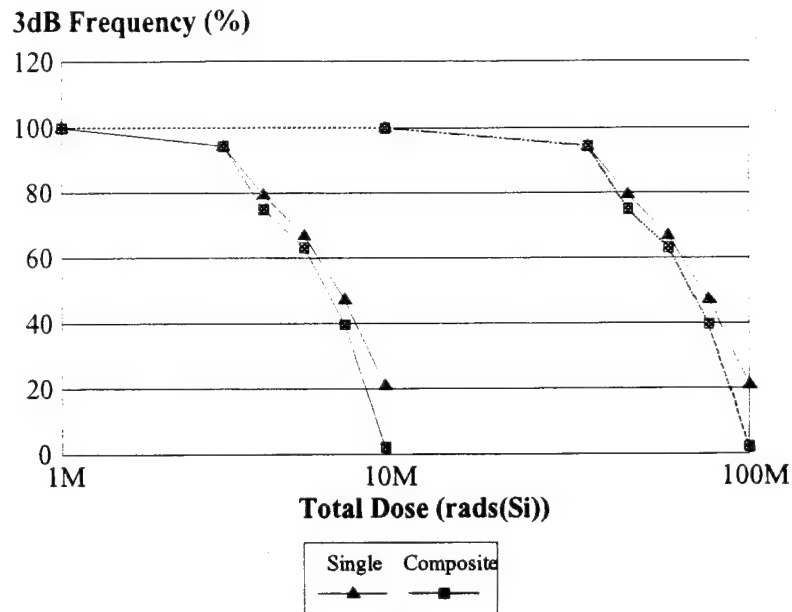


Figure 8.4 BJT Composite and Single Op Amp Percent 3dB Frequency versus Total Dose

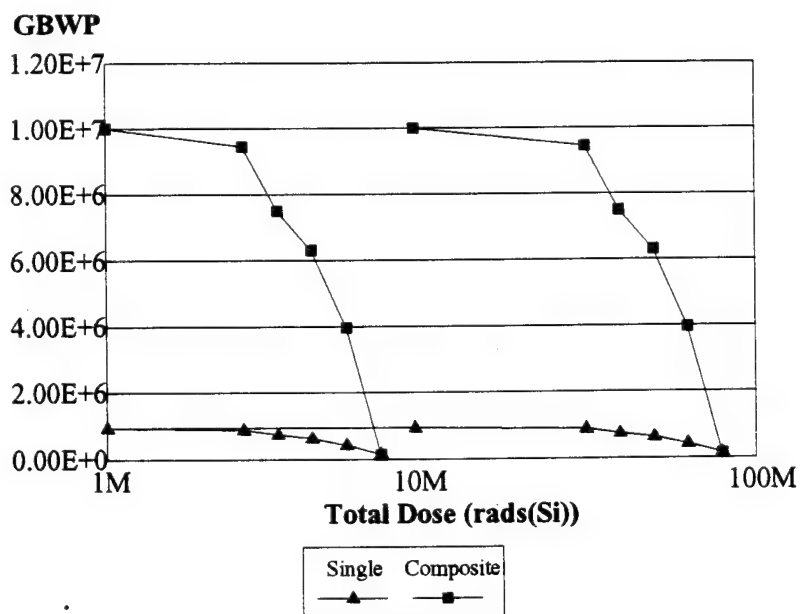


Figure 8.5 BJT Composite and Single Op Amp Gain Bandwidth Product (GBWP) versus Total Dose

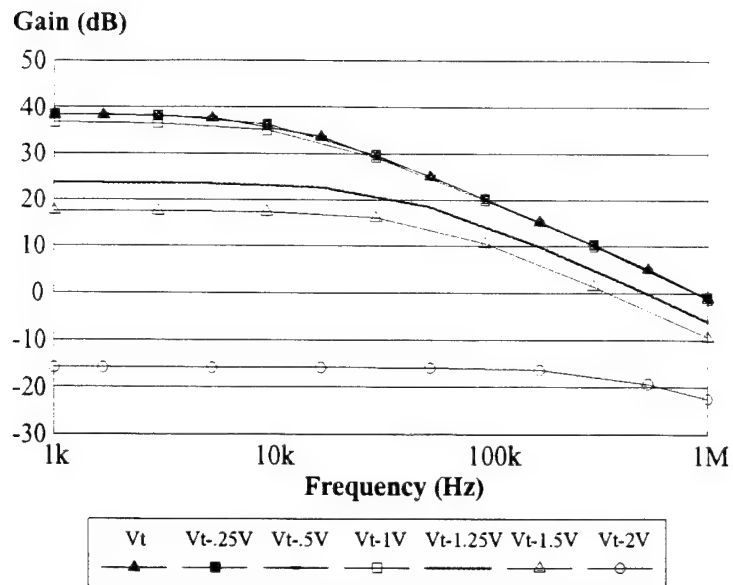


Figure 8.6a CMOS Single Op Amp Gain Degradation Curves versus Frequency as a Function of Threshold Voltage

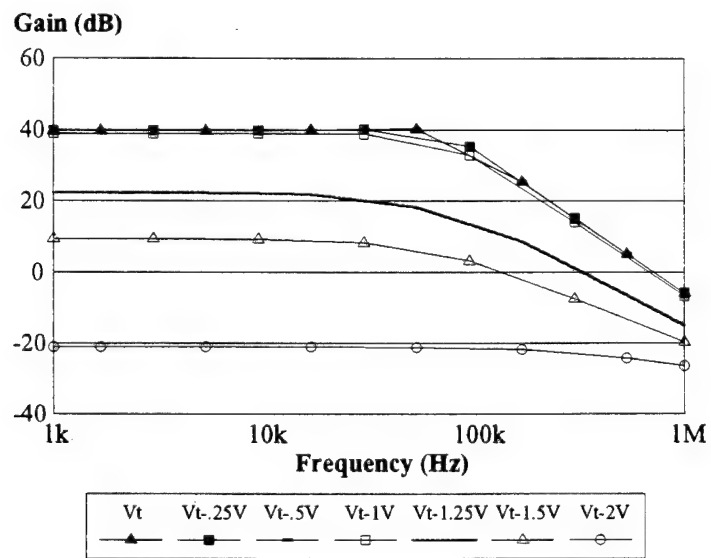


Figure 8.6b CMOS Composite Op Amp Gain Degradation Curves versus Frequency as a Function of Threshold Voltage

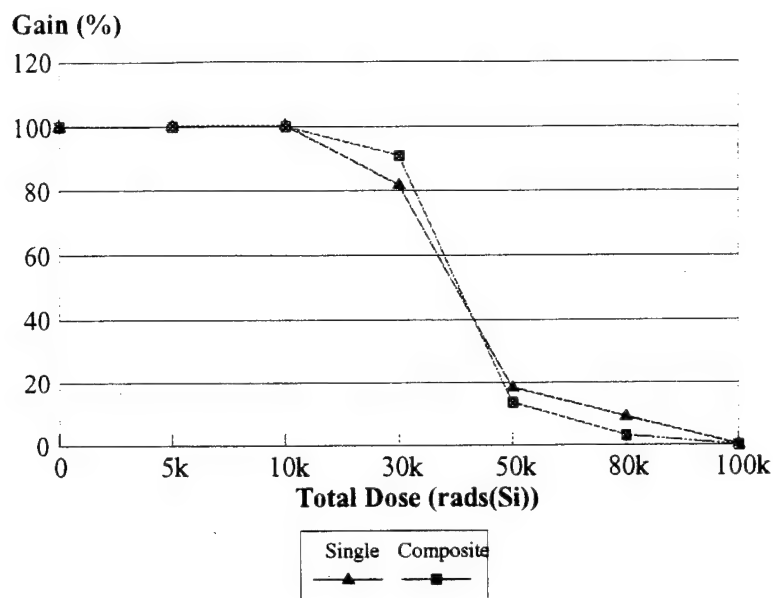


Figure 8.7 CMOS Composite and Single Op Amp Gain versus Total Dose

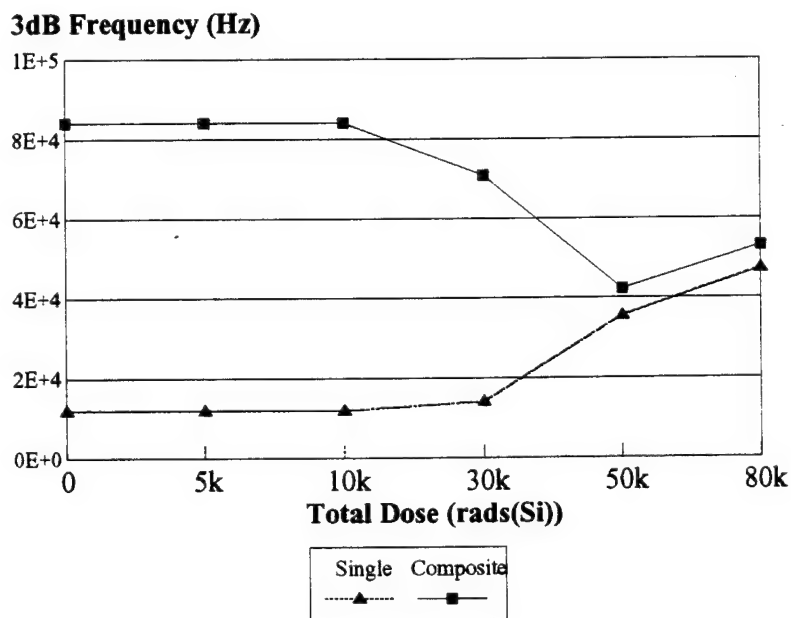


Figure 8.8 CMOS Composite and Single Op Amp 3dB Frequency versus Total Dose

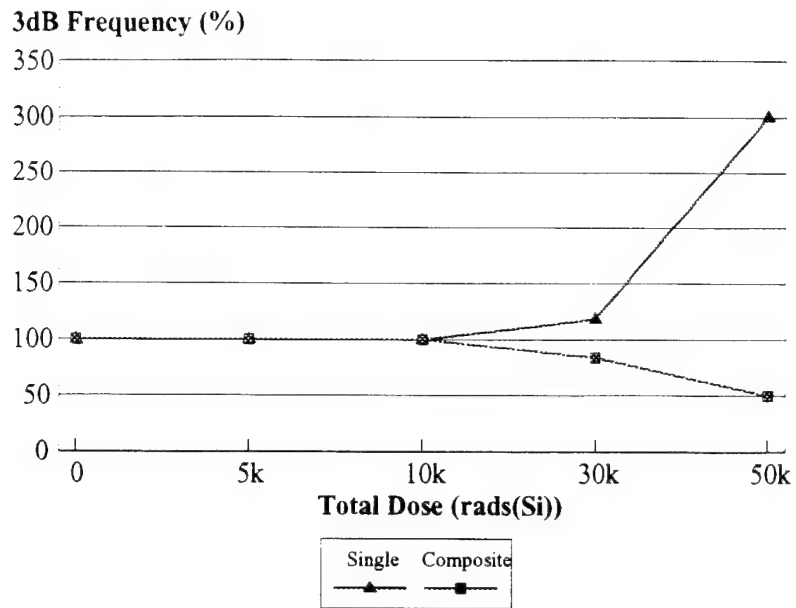


Figure 8.9 CMOS Composite and Single Op Amp 3dB Frequency versus Total Dose

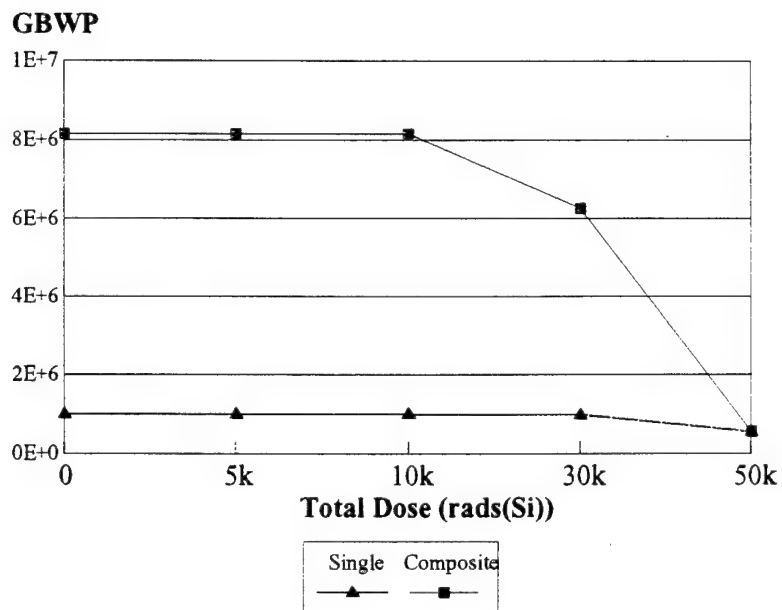


Figure 8.10 CMOS Composite and Single Op Amp Gain Bandwidth Products (GBWP) versus Total Dose

Figure 8.11 displays the maximum slewrate for each degradation point of the BJT circuits; again, the twin curves are an outgrowth of  $\beta$ -to-total-dose mapping using Figure 4.2. Comparing Figures 8.12 and 8.13, it is interesting to see that the BJT single op amp experienced only a decrease in slewrate for increasing total dose, whereas the BJT composite op amp experienced a decrease in slewrate accompanied by delays. The slewrate results of the CMOS circuits depicted in Figures 8.14 through 8.16 parallel and confirm those of the BJTs, except for the lower total dose threshold.

## **B. COMPARISON WITH LINAC RESULTS**

### **1. Non Rad Hard Op Amp Comparison**

This simulation was originally intended only for comparison with the non rad hard component data of Figure 6.1. The thought was that, due to the simplicity of the modeled op amps, the radiation response of the basic, inexpensive, non rad hard op amps would compare better than that of the complex, costly, rad hard op amps. Hence, the non rad hard data was primarily the focus of attention. Referring to Figure 6.1, the relative gain loss versus total dose compared fairly well with the lower boundary curve of the simulation results in Figure 8.2. Both sets of gains started decreasing around 3M rads(Si) (Figure 8.2 is pseudo-logarithmic), with a slightly steeper gain degradation rate thereafter for the LINAC op amps (Sage's data). The 3dB frequency and slewrate data, however, did not compare well. While the previous results showed a marked difference of approximately 25% in percent 3dB frequency between the single and composite op amps, the simulated response in Figure 8.4 showed, idealistically, no difference in the two.

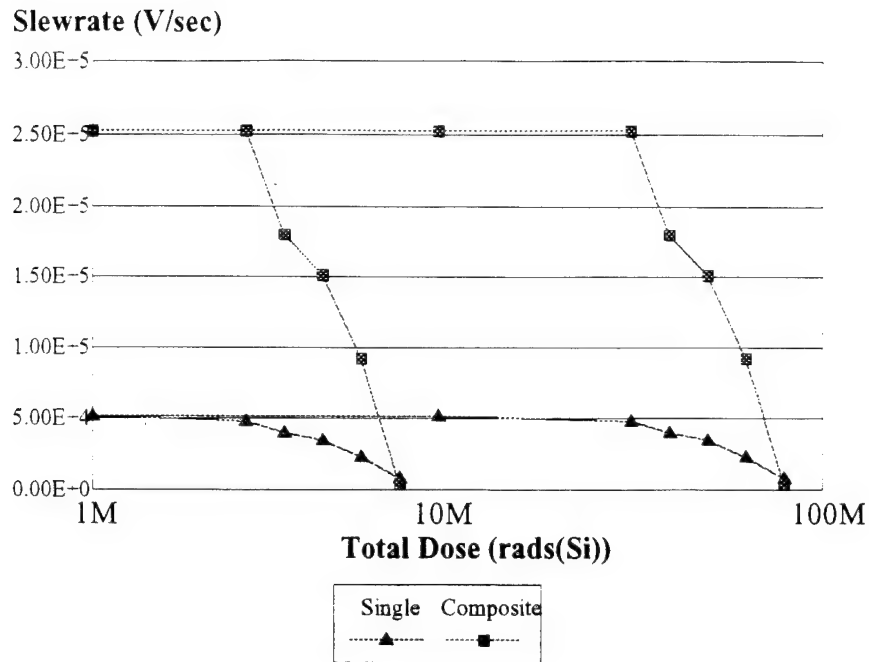


Figure 8.11 BJT Composite and Single Op Amp Slewrate versus Total Dose

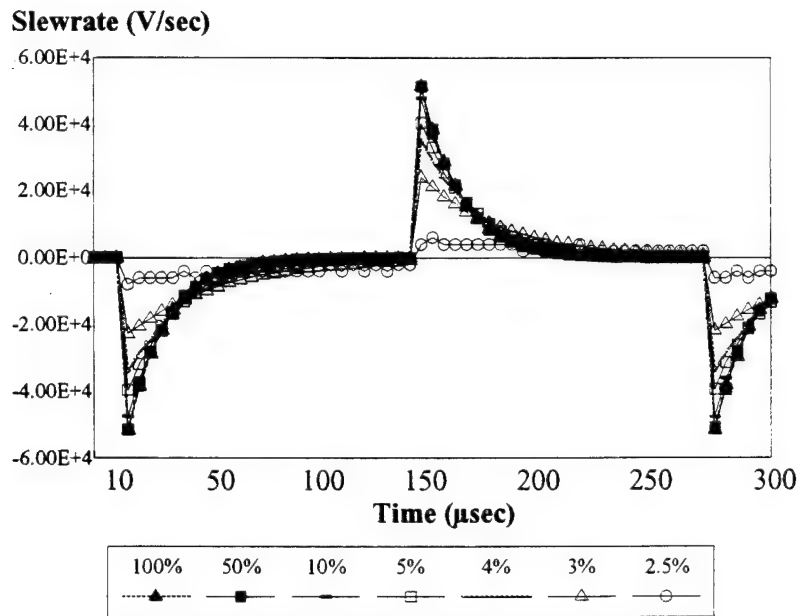


Figure 8.12 BJT Single Op Amp Slewrate Degradation Curves versus Time as a Function of Percent Remaining Beta

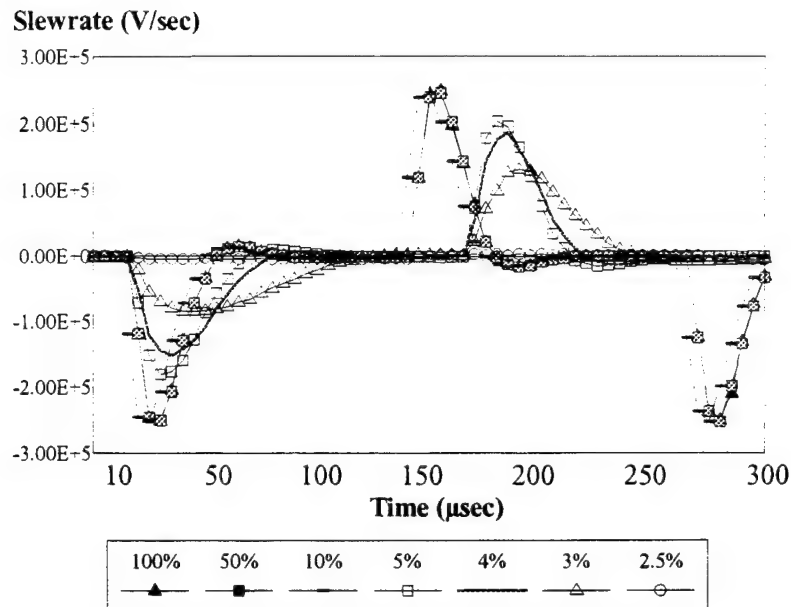


Figure 8.13 BJT Composite Op Amp Slewrate Degradation Curves versus Time as a Function of Percent Remaining Beta

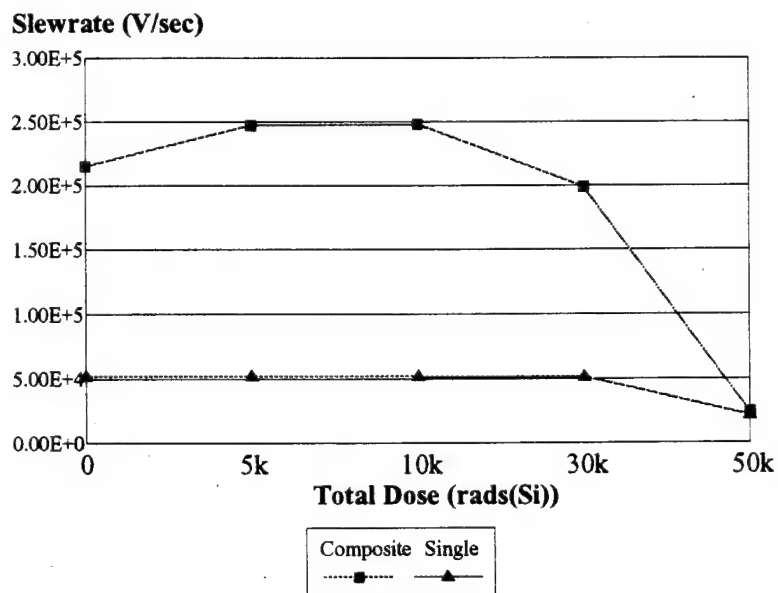


Figure 8.14 CMOS Composite and Single Op Amp Slewrate versus Total Dose

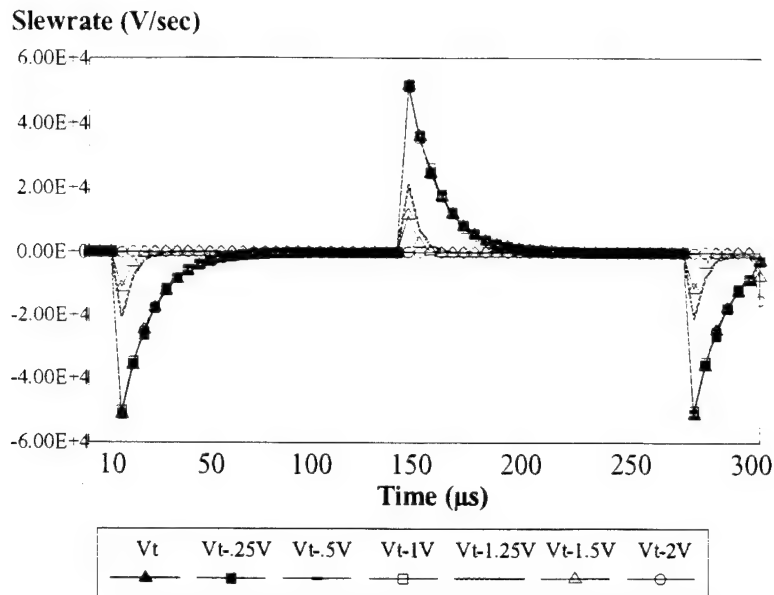


Figure 8.15 CMOS Single Op Amp Slewwrate Degradation Curves versus Time as a Function of Percent Remaining Beta

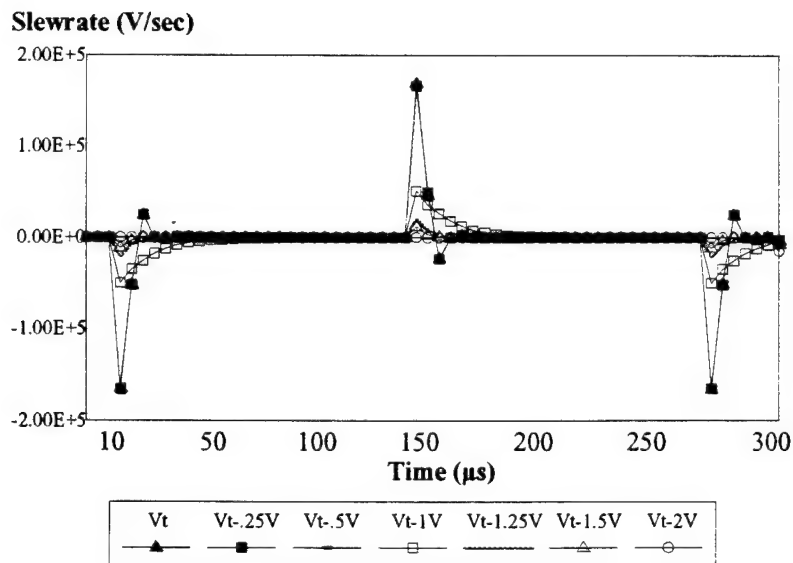


Figure 8.16 CMOS Composite Op Amp Slewwrate Degradation Curves versus Time as a Function of Percent Remaining Beta



Additionally, 30-60% 3dB frequency decrease was witnessed prior to 1M rads(Si), where the simulated results revealed no decrease until approximately 3M rads(Si).

## **2. Rad Hard Op Amp Comparison**

The above results were somewhat depressing. After reinvestigating all models and programs to check for any error which would cause such a discrepancy in response, it was decided that the reason why the data did not compare very well was due to the fact that the modeled op amps were very different than those that were experimentally irradiated in the LINAC, and would be expected to respond differently. However, due to a sudden and unexpected arabesque analytical leap, it was determined that this thinking was wrong: the simplicity of the simulation yields an ideal response to ionizing radiation, so the more ideal the component which the simulation is to be compared with, or the more rad hard the component, the closer the results would be. Hence, a rad hard op amp comparison was included as well.

Referring to Figures 6.2 and 6.3 for 18M rads(Si) and 68M rads(Si) exposure, respectively, the comparison improved considerably with Figure 6.2 in that all three op amps irradiated to 18M rads(Si) fell just within the normalized gain and 3dB frequency versus total dose windows in Figures 8.2 and 8.4. Figure 6.3 data, where the op amps were irradiated to 68M rads(Si), proved to be an even better comparison, because the data fell in the middle of the above-mentioned windows.

## IX. CONCLUSIONS AND RECOMMENDATIONS

There are two conclusions that may be gleaned from all of this. First and foremost is that composite op amps are faster and provide a broader operational bandwidth relative to single op amps.

The second conclusion is that the more rad hard the component is to be modeled, the better the prediction of its response to total dose radiation will be as a result of this simulation method. Characteristics which rad hard devices may be immune to, such as stray capacitances, noise, structure, surface conditions, etc., which are difficult to predict, were not simulated. However, these characteristics may drive a significant portion of the non rad hard component response, so much so that this model simulation method is not very useful in predicting non rad hard response to total dose radiation.

Additionally, it is hard to believe that even rad hard BJT devices can still operate after exposure to 50M rads(Si), as this is equivalent to 50 years in the densest regions of the Van Allen Belts. We may never know whether this is actually true, since other satellite subsystems, particularly batteries and propellant, do not last that long. However, the results of this simulation stand behind the results of the LINAC irradiation.

In order to fully understand the relationship between transistor response and op amp circuit response, a recommendation for future work is to irradiate a chip containing transistors and at least one op amp made from those same transistors. Measurements of the responses in these experiments have to also be obtained in-situ in order to avoid annealing effects. Upon conducting such an experiment, a comparison could be

performed of the measured output from the irradiated op amp model with the predicted response of the op amp using this simulation procedure, but with new transistor parameter degradation values extracted from the in-situ transistor measurements.

## REFERENCES

1. Tabbert, Chuck. "A Historical Perspective," The Space Radiation Environment, Harris Semiconductor, Melbourne, Florida, September 1993.
2. Rivet, Steve. "Space Radiation Environments," The Space Radiation Environment, Harris Semiconductor, Melbourne, Florida, September 1993.
3. Messenger, G.C. and Ash, M.S. The Effects of Radiation on Electronic Systems, Van Nostrand Reinhold Company, Inc., New York, New York, September 1986.
4. Rivet, Steve and Clark, Jack. "Radiation Effects on Integrated Circuits," The Space Radiation Environment, Harris Semiconductor, Melbourne, Florida, September 1993.
5. Sedra, Adel S. and Smith, Kenneth C. Microelectronic Circuits, Third Edition, Saunders College Publishing, Chicago, Illinois, 1991.
6. Mikhael, Wasfy B. and Michael, Sherif, "Composite Operational Amplifiers: Generation and Finite-Gain Applications," IEEE Trans. Circuits and Systems, CAS-34, No. 5, pp.461-470, May 1987.
7. Mikhael, Wasfy B. and Michael, Sherif, "Inverting Integrator and Active Filter Applications of Composite Operational Amplifiers," IEEE Trans. Circuits and Systems, CAS-34, No. 5, pp.449-460, May 1987.
8. Lohr, David Michael, A Technique for Improving Active Network Performance in a Radiation Environment Without the Use of Hardened Devices, Master's Thesis, Naval Postgraduate School, Monterey, California, March 1987.
9. Michael, Sherif, Composite Operational Amplifiers and Their Application in Active Networks, Doctoral dissertation, West Virginia University, Morgantown, West Virginia, 1983.
10. Gariano, Patrick Jr., Generation of an Optimum High Speed High Accuracy Operational Amplifier, Master's Thesis, Naval Postgraduate School, Monterey, California, September 1985.
11. Sage, Scott Edward, Total Dose Radiation Effects on Bipolar Composite and Single Operational Amplifiers Using a 30MeV Linear Accelerator, Master's Thesis, Naval Postgraduate School, Monterey, California, June 1988.

12. Larin, Frank, Radiation Effects in Semiconductor Devices, John Wiley & Sons, New York, New York, 1968.
13. DeLaus, Michael, "Radiation Concerns in State-of-the-Art Processing Technologies," 1994 IEEE NSREC Short Course, Tucson, Arizona (July 1994).
14. Measel, Wasfy B. and Brown, Sherif, "Inverting Integrator and Active Filter Applications of Composite Operational Amplifiers," IEEE Trans. Circuits and Systems, CAS-34, No. 5, pp.449-460, May 1974.
15. Lint, Wasfy B. and Michael, Sherif, "Inverting Integrator and Active Filter Applications of Composite Operational Amplifiers," IEEE Trans. Circuits and Systems, CAS-34, No. 5, pp.449-460, May 1974.
16. Pease, Ronald L., Johnston, Allan H., and Azarewicz, Joseph L., "Radiation Testing of Semiconductor Devices for Space Electronics," Proceedings of the IEEE, vol 76, No. 11, pp.1510-1526, November 1988.
17. Pease, Ronald L., Johnston, Allan H., and Azarewicz, Joseph L., "Radiation Testing of Semiconductor Devices for Space Electronics," Proceedings of the IEEE, vol 76, No. 11, pp.1510-1526, November 1988.
18. Halliday, David, and Resnick, Robert, Fundamentals of Physics, ed. 3, John Wiley & Sons, New York, New York, 1988.
19. Rudie, Norman J., Principles and Techniques of Radiation Hardening, vols III, IV, and V, Western Periodicals Co., North Hollywood, California, 1986.
20. Winokur, Peter S., "Total-Dose Radiation Effects," IEEE Nuclear and Space Radiation Effects Conference Short Course, New Orleans, Louisiana, July 13, 1992.

## INITIAL DISTRIBUTION LIST

- |    |                                                                                                                                                 |   |
|----|-------------------------------------------------------------------------------------------------------------------------------------------------|---|
| 1. | Defense Technical Information Center<br>Cameron Station<br>Alexandria, VA 22304-6145                                                            | 2 |
| 2. | Library, Code 52<br>Naval Postgraduate School<br>Monterey, CA 93943-5101                                                                        | 2 |
| 3. | Chairman, Code EC<br>Department of Electrical and Computer Engineering<br>Naval Postgraduate School<br>Monterey, CA 93943-5121                  | 1 |
| 4. | Professor S. Michael, Code EC/Mi<br>Department of Electrical and Computer Engineering<br>Naval Postgraduate School<br>Monterey, CA 93943-5121   | 2 |
| 5. | Professor R. Panholzer, Code EC/Pz<br>Department of Electrical and Computer Engineering<br>Naval Postgraduate School<br>Monterey, CA 93943-5121 | 1 |
| 6. | LT Rebecca L. Baczuk<br>3690 Golden Hills Ave<br>S.L.C., UT 84121                                                                               | 2 |